RESEARCH ARTICLE

Microbiome profiling in extremely acidic soils affected by hydrothermal fluids: the case of the Solfatara Crater (Campi Flegrei, southern Italy)

Simona Crognale[1], Stefania Venturi[2,3], Franco Tassi[2,3], Simona Rossetti[1], Heba Rashed[3], Jacopo Cabassi[2,3], Francesco Capecchiacci[2,3], Barbara Nisi[4], Orlando Vaselli[2,3], Hilary G. Morrison[5], Mitchell L. Sogin[5] and Stefano Fazi[1,*]

[1]IRSA - CNR Water Research Institute, Via Salaria km 29.300 – CP10, 00015 Monterotondo, Rome, Italy, [2]IGG – CNR Institute of Geosciences and Earth Resources, Via G. La Pira 4, 50121 Florence, Italy, [3]Department of Earth Sciences, University of Florence, Via G. La Pira 4, 50121 Florence, Italy, [4]IGG – CNR Institute of Geosciences and Earth Resources, Via G. Moruzzi 1, 56124 Pisa, Italy and [5]Marine Biological Laboratory, Woods Hole, MA, USA

*Corresponding author: CNR – IRSA Water Research Institute, Via Salaria km 29.300 – CP10, 00015 Monterotondo, Rome, Italy. Tel: +390-690672790; E-mail: fazi@irsa.cnr.it

One sentence summary: The geochemical and microbiological characterization of extremely acidic soils from the Solfatara Crater highlighted how the microbial communities are shaped by deep-originated gases and elements.

Editor: Gary King

ABSTRACT

An integrated geochemical and microbiological investigation of soils from the Solfatara Crater (Campi Flegrei, southern Italy) demonstrated that interstitial soil gases dominated by CO_2 and other typical hydrothermal gaseous species (e.g. H_2S, CH_4, ethane, benzene, alkenes and S-bearing organic compounds) influenced the composition of microbial communities. The relatively high concentrations of hydrothermal fluids permeating the soil produced acidic conditions and whitish deposits that characterize the Solfatara Crater floor. Archaea and Bacteria showed almost equal cell abundance (up to 3.2×10^7 and 4.2×10^7 cell/g, respectively) with relatively low levels of biodiversity and equitability in sites characterized by elevated temperatures (up to 70°C), very low pH values (up to 2.2) and reducing conditions. In these sites, high-throughput sequencing showed the marked selection of microorganisms, mainly affiliated with the genera *Thermoplasma*, *Ferroplasma* and *Acidithiobacillus*. A relatively high biodiversity and concomitant distinctive structure of the microbial community were observed in soils poorly affected by fumarolic emissions that were oxic and rich in organic matter.

Keywords: microbiome; hydrothermal fluids; soil; sediment; solfataric field; Campi Flegrei

INTRODUCTION

During the last few decades, studies in hydrothermal, geothermal and anthropogenic high-temperature ecosystems have discovered previously unknown diversity of thermophilic microorganisms (Huber, Huber and Stetter 2000; Menzel *et al.* 2015; Colman *et al.* 2018). Genomic studies of thermophilic microbes inhabiting these extreme environments have predicted numerous microbial metabolic pathways directly involved in key global processes such as nutrient (e.g. C, N, S, Fe) and trace element (e.g. As, Sb, Hg) cycling and gas exchange (CO_2 and CH_4) (Inskeep *et al.* 2013). Solfataric fields, characterized by low pH

and high temperatures, represent one of the most extreme environments widespread on Earth (e.g. Krisuvik, Hveragerthi and Kerlingarfjöll, Iceland; Yellowstone National Park, USA; White Island, New Zealand; the Kamchatka Peninsula, Russia; Hokkaido, Japan; and Campi Flegrei, Italy).

Solfatara Crater is a relatively young tuff cone (ca. 4000 yr BP) located in the town of Pozzuoli, a few km west of Naples (southern Italy). It represents the most prominent surface hydrothermal manifestation in the Campi Flegrei caldera. It is characterized by the occurrence of a relatively strong emission of hydrothermal fluids, mainly consisting of water vapor and CO_2 (Chiodini *et al.* 1998; Chiodini *et al.* 2001; Caliro *et al.* 2007; Chiodini *et al.* 2010; Tassi *et al.* 2015a) and significant amounts of CH_4, H_2S, C_6H_6 and gaseous elemental mercury (GEM) in both fumarolic fluids and soils (Tassi *et al.* 2013, 2015a, 2016; Sicola *et al.* 2015). Steam condensation at shallow depths produces significant thermal anomalies and hot soils in the Solfatara Crater, which was known to the Romans as the *Forum Vulcani* (in Latin: *home of the god of fire*), as in Strabone's *Strabonis geographica*. Hydrothermally altered soils carpet the crater floor that includes native sulfur, sulfate and sulfide encrustations, alunite and amorphous silica. Anomalous enrichments in deep-originated elements, e.g. K, Cs, Sb, Cl, F and Sr, were also recognized (Allard *et al.* 1991; Bruno *et al.* 2007; Sgavetti *et al.* 2009; Piochi *et al.* 2015; Mayer *et al.* 2016). The Solfatara soils exhibit a typical whitish color induced by intense hydrothermal alteration of the volcanic rocks under acidic conditions (Turney *et al.* 2008; Piochi *et al.* 2015). The altered deposits progressively turn grayish approaching the central part of the Solfatara Crater, named *Fangaia* (an Italian term to define a muddy zone), which hosts bubbling acidic mud pools that form through interactions of rainwater, steam condensation and hydrothermal gases. This area, as well as the north- and south-eastern fumarolic fields, shows the highest soil temperatures (Chiodini *et al.* 2001). In contrast, Mediterranean maquis, with holms and oaks, strawberry trees and pines, covers the north-western portion of the crater with no significant heat and gas flux anomalies (e.g. Tassi *et al.* 2013, 2016). Recent monitoring of the Solfatara Crater within the Campi Flegrei caldera has shown increasing seismic and deformation activity and significant chemical variations of the fumarolic gas discharges (Chiodini *et al.* 2016, 2017; Kilburn *et al.* 2017).

The chemical characterization of the Solfatara volcano and the entire Campi Flegrei has been thoroughly documented (e.g. Tassi *et al.* 2013; Chiodini *et al.* 2015a; Cardellini *et al.* 2017; Montanaro *et al.* 2017; Venturi *et al.* 2017a), but little is known about the microorganisms living in these extreme environments. A previous low-throughput molecular analysis of the bacterial composition of soil and crust samples collected near the fumarolic vents and the acidic mud pools in the center of the Solfatara Crater identified the presence of bacteria mainly affiliated with *Proteobacteria*, *Acidobacteria* and *Actinobacteria* (Glamoclija *et al.* 2004a). The analysis revealed the occurrence of thermophilic or thermotolerant iron and hydrogen oxidizers or methane/methanol consumers, although many phylotypes were too distantly related to cultivated species to infer potential metabolic properties (Glamoclija *et al.* 2004a). To understand the adaptive strategies and the ecological role of the microbial communities in these acidic and high-temperature environments, it is important to identify those metabolic features that allow them to thrive in these extreme conditions.

Our study focused on profiling at high resolution both the archaeal and bacterial components of high-temperature and extremely acidic soils in the Solfatara Crater by combining results of next generation sequencing (NGS) with single-cell quantification assays. The study plan also included the integration of geochemical and microbiological data to develop an overview of soil community composition in relation to different degrees of enrichment in deep-origin gases and elements.

MATERIALS AND METHODS

Study site: Solfatara Crater

The Solfatara Crater (Fig. 1) hosts one of the largest fumarolic discharges worldwide (mostly represented by Bocca Grande and Bocca Nuova fumaroles), whose associated thermal energy flux was estimated to be ∼100 MW (Chiodini *et al.* 2001). Most thermal energy is released by widespread diffuse degassing fed by a 1.5–2 km deep column of an ascending mixture of (i) magmatic gases (about 26%) released by the degassing of a magma body at ∼5 km depth (Gottsmann, Rymer and Berrino 2006) and (ii) hydrothermal fluids (about 74%) originated by the boiling of overlying aquifer(s) (e.g. Chiodini *et al.* 2001; Caliro *et al.* 2007; Chiodini *et al.* 2015b; Cardellini *et al.* 2017). Whilst fumarolic activity is mainly restricted to the south- and north-eastern sectors of the crater, diffuse degassing is widespread and anomalous soil CO_2 fluxes nearly affect the entire bottom of the crater. According to Cardellini *et al.* (2017), a total soil CO_2 output varying from 1116 ± 138 to 1524 ± 164 tons/day was recorded in 2012–2013, which is comparable to the CO_2 flux associated with a 'medium-large' volcanic plume from persistently degassing volcanoes such as Soufrière Hills or Mount Erebus (Burton, Sawyer and Granieri 2013; Cardellini *et al.* 2017).

In January 2016, five soil-sampling sites at the Solfatara Crater were selected together with two acidic mud pools in the Fangaia area for biogeochemical investigations (Fig. 1). The selection of the sites for collecting soil and mud samples was based on field measurements of temperature and diffuse CO_2 flux. Soil samples were collected at 10 and 30 cm depth for subsequent analyses. The soil samples strongly affected by fumarolic gas emissions (S1, S2, S3) were characterized by a whitish coverage typically produced by sulfuric acid. Sampling sites S4 and S5 were collected from hydrothermalized terrains far from fumarolic emission and covered by typical Mediterranean vegetation. Muds S6 and S7 were sampled from the acidic Fangaia mud pools.

Sampling methods and field measurements

At each site, diffuse CO_2 (ΦCO_2) and CH_4 (ΦCH_4) fluxes from the soil were measured according to (i) the 'accumulation chamber (AC) method' (Chiodini *et al.* 1998) and (ii) the 'static closed-chamber (SCC) method' (Tassi *et al.* 2013), respectively. Equipment and procedures are described in Tassi *et al.* (2015a). Interstitial soil gases were collected from sites S1 to S5 by inserting a 1 m-long stainless steel tube down to the sampling depth (10 and 30 cm at each site). At 10 and 30 cm the soil temperature was measured with a Thermocouple Sensor K 3K350. The soil gases were stored in two 12 cm^3 Labco Exetainer® glass vials, equipped with a porous membrane, for subsequent chemical and isotopic analysis. The sampling procedure is described in Tassi *et al.* (2015b). Soil samples for chemical and microbiological analyses were collected at 10 and 30 cm depth using sterilized spoons. Aliquots for microbiological analyses were immediately fixed with formaldehyde solution (final concentration 1%) and stored at 4°C for total cell counts and fluorescence *in situ* hybridization. Aliquots of 15 mL for DNA extraction were placed
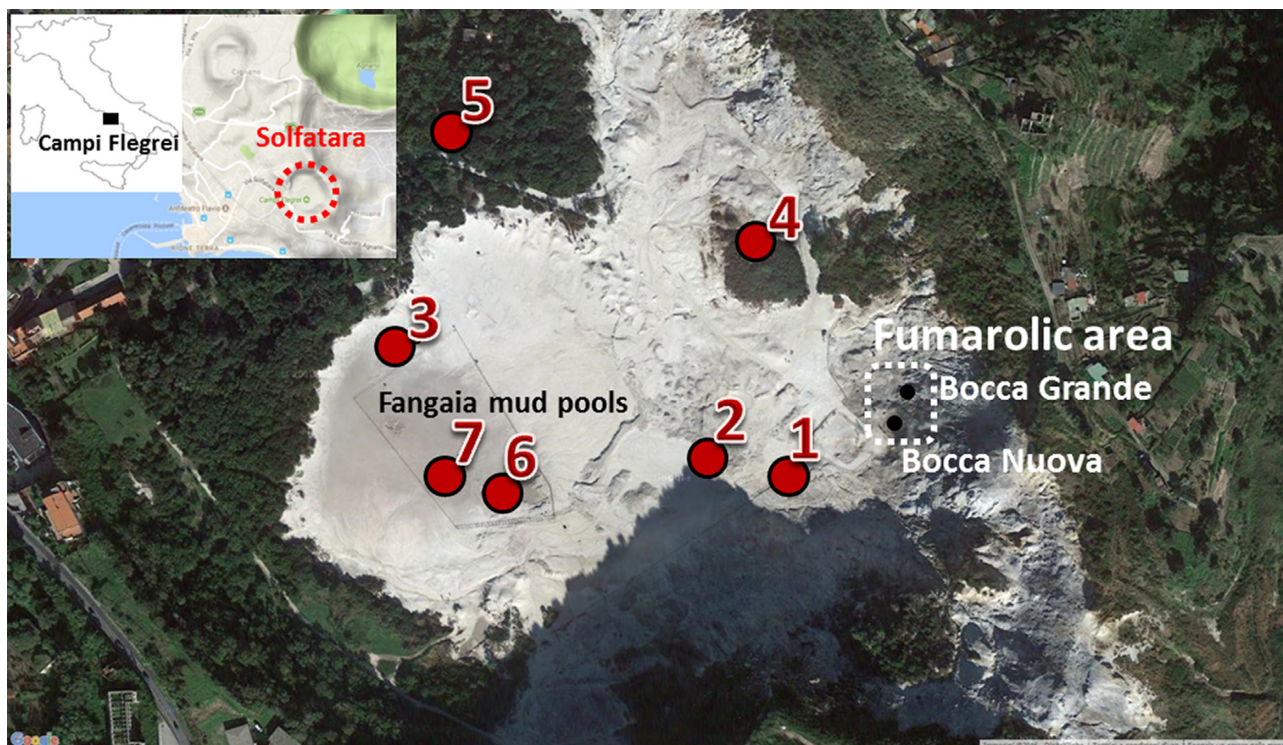
Figure 1. Map of the Solfatara Crater in Campi Flegrei caldera (Italy) with the location of sampling sites (1–7) and Bocca Grande and Bocca Nuova fumaroles.

in dry ice immediately after collection and then stored in the laboratory at -20°C until further processing. Soil samples for chemical analyses were stored and sealed in plastic bags.

Bubbling gases from sites S6 and S7, i.e. the Fangaia mud pools, were conveyed to a pre-evacuated 60 mL glass flask, equipped with a Thorion® valve and containing 20 mL of 4 M NaOH solution (Giggenbach 1975), using an inverted funnel positioned above the bubbles. A glass vial for the analysis of volatile organic compounds (VOCs) was also collected. Water samples from the mud pools were filtered at 0.45 μm and collected in 125 mL polyethylene bottles. Temperature, pH and Eh (Redox potential) of pool waters were measured *in situ*. Mud samples for chemical and microbiological analyses were collected from the pools by plastic bags and sterilized tubes, respectively. Mud aliquots for microbiological and chemical analyses were preserved as described for soil samples.

Chemical and isotopic analyses of gas samples

Inorganic gases both in the headspace of the bubbling pool sampling flasks (N_2, O_2, H_2, Ar, CO) and in the glass vials (CO_2, H_2S, N_2, O_2, Ar) were analyzed using a Shimadzu 15A gas chromatograph (GC) equipped with a thermal conductivity detector (TCD) and a 10 m-long 5A Molecular Sieve column or, for CO_2 and H_2S analysis in the glass vials, a 3 m-long column packed with Porapak Q 80/100 mesh. Light hydrocarbons (C_1-C_3) were analyzed using a Shimadzu 14A gas chromatograph equipped with a Flame Ionization Detector (FID) and a 10 m-long stainless steel column packed with Chromosorb PAW 80/100 mesh coated with 23% SP 1700. CO_2 and H_2S dissolved in the alkaline solution of the flasks were analyzed as CO_3^{2-} by automatic titration (AT) with 0.5 M HCl solution (Metrohm 794 Basic Titrino) and SO_4^{2-} by ion chromatography (Metrohm 761 Compact IC) after oxidation with H_2O_2 (Montegrossi *et al.* 2001; Vaselli *et al.* 2006). VOCs were analyzed, after Solid Phase Micro Extraction (SPME; Arthur and

Pawliszin 1990), by using a Thermo Trace GC Ultra gas chromatograph coupled to a Thermo DSQ Quadrupole Mass Spectrometer. The SPME and analytical procedures are described in Tassi *et al.* (2015a), together with instrumental specifications. Analytical errors for AT, GC and IC were <5%.

The $^{13}C/^{12}C$ ratios in CO_2 (expressed as $\delta^{13}C$-CO_2 ‰ V-PDB (Vienna Pee Dee Belemnite)) were determined by using a Finningan Delta Plus mass spectrometer after a two-step extraction and purification procedure of the gas mixtures by using liquid N_2 and a solid-liquid mixture of liquid N_2 and trichloroethylene (Evans, White and Rapp 1998; Vaselli *et al.* 2006). Internal (Carrara and San Vincenzo marbles) and international (NBS18 and NBS19) standards were used for estimation of external precision. The analytical uncertainty and the reproducibility were ± 0.05‰ and ± 0.1‰, respectively.

Chemical analysis of soil, mud and water samples

Soil and mud samples were dried at 40°C for 48 h, sieved at 2 mm and grinded with a planetary agate ball mill until an impalpable powder was obtained. Loss On Ignition (L.O.I.), i.e. the total volatile content, was determined by gravimetry. The powdered sample was dried at 110°C for 8 h, weighted (dry weight) and heated at 950°C for 2 h using a CEM microwave oven. The L.O.I. values were expressed as percentage by weight. The bulk chemical composition of soil samples was analyzed by X-ray fluorescence (XRF) on pressed powder pellets using a Rigaku II wavelength dispersive spectrometer equipped with a Rh anode at CRIST (Center of Structural Crystallography, University of Florence). The composition of the main and trace elements was acquired using a ZSX Rigaku Software Package version 3.50 and determined with the SQX semi-quantitative element analysis routine. The Fundamental Parameter (FP) software was used

to allow elemental quantification of the samples without standards.

The pH of the soils was potentiometrically measured in the supernatant suspension of a 1:2.5 soil:KCl (1 M) solution mixture (Peech 1965; ISRIC 1995). For each sample, 10 g of soil were amended with 25 mL of KCl 1 M solution. Before measuring the pH, the obtained mixture was shacked for 2 h and then centrifuged at 5000 rpm for 5 min.

Soluble elements were determined through H_2O extraction by adding 100 mL of MilliQ water to 5 g of soil and mud samples and mechanically stirring overnight for 8 h. The final solution, obtained by filtering (0.45 μm) the leachate, was acidified by adding 1 mL of Suprapur® HNO_3 and analyzed by ICP-OES using a PerkinElmer Optima 8000 (PerkinElmer, Waltham, MA) for Mn, Fe, Co, Ni, Cu, Zn, As, Sb, Al, Hg, W, Si, Pb, P and Cd. The analytical error was <10%.

Water samples from the Fangaia pools were analyzed by ion-chromatography using an 861 Advanced Compact IC-Metrohm for cations (Na, K, Mg, Ca and Li) and a 761 Compact IC-Metrohm for anions (F, Cl, Br, SO_4 and NO_3). The analytical error was <3%.

Total prokaryotic abundance, CARD-FISH and NGS

The total prokaryotic abundance was estimated by DAPI staining, and Bacteria and Archaea abundances by Catalyzed Reported Deposition-Fluorescence *in situ* Hybridization (CARD-FISH) following the protocol optimized by Fazi, Amalfitano and Pizzetti (2007), and Fazi *et al.* (2013). Specific rRNA-target horseradish peroxidase (HRP)-labeled oligonucleotidic probes (Biomers, Ulm, Germany) targeted Bacteria (EUB338 I-III) and Archaea (ARCH915). Details of the probes are available at probe-Base (Greuter *et al.* 2016). The stained filter sections were inspected on a Leica DM LB30 epifluorescence microscope (Leica Microsystems, Wetzlar, Germany) at 1000X magnification. At least 300 cells were counted in >10 microscopic fields randomly selected across the filter sections. The relative abundance of hybridized cells was estimated as the ratio of hybridized cells to total DAPI-stained cells.

DNA was extracted from 1 g of soil and mud samples. The extraction was performed with PowerSoil® DNA Isolation Kit (MoBio, Carlsbad, CA) according to the manufacturer's instructions. The genomic DNA samples were quantified using PicoGreen (ThermoFisher Scientific). DNA was stored at -20°C in small aliquots.

Bacterial/Archaeal 16S rRNA gene sequencing libraries were prepared by the Marine Biological Laboratory (MBL, Woods Hole, MA) in the framework of Census of Deep Life Sequencing Opportunities 2016. The v4v5 regions of the 16S rRNA gene were amplified separately for bacteria and archaea. Bacterial 16S rRNA gene was amplified in triplicate using primers 518F (5'- CCAGCAGCYGCGGTAAN -3') and a combination of three reverse primer variants 926R (5'- CCGTCAATTCNTTTRAGT CCGTCAATTTCTTTGAGT CCGTCTATTCCTTTGANT -3') as previously described (Huse *et al.* 2014a). The archaeal v4v5 16S rRNA gene was amplified in triplicate by using a combination of five forward primer variants (517F; GCCTAAAGCATC-CGTAGC, GCCTAAARCGTYCGTAGC, GTCTAAAGGGTCYGTAGC, GCTTAAAGNGTYCGTAGC, GTCTAAARCGYYCGTAGC) and a single reverse primer (958R; CCGGCGTTGANTCCAATT) (Topçuoğlu *et al.* 2016). The amplification products were visualized on a Caliper High Sens assay (Perkin Elmer, Waltham, MA), quantified by PicoGreen assay (Life Technologies, Grand Island, NY) and pooled in equimolar concentrations. The pool was sequenced as paired-end 250 cycle reads on the Illumina Miseq (Illumina,

San Diego, CA). The sample datasets were demultiplexed using a combination of Miseq Reporter software and custom python scripts. Data processing and diversity analyses were performed at the MBL. Specifically, paired reads were merged to produce high-quality full-length v4v5 sequences and the taxonomic affiliation of each unique sequence was assigned using GAST (Huse *et al.* 2008). GAST assigns taxonomy based on the results of VSEARCH (Rognes *et al.* 2016). Alignments must cover 80% of the read length and 66% of the matched sequences must share the same taxonomic string. If the reference taxonomies are discordant, the assignment is moved up a taxonomic level until two-thirds consensus is reached. Sequences that shared the same taxonomic assignment were grouped into operational taxonomic units (OTUs). The results were uploaded to the Visualization and Analysis of Microbial Population Structures (VAMPS) website (http://vamps.mbl.edu; Huse *et al.* 2014b). Downstream analyses used OTUs that were comprised of tags having the same taxonomic assignment.

Statistical analysis

The non-parametric Mann-Whitney U test was applied to verify the statistical differences between strongly and not-strongly affected samples by hydrothermal fluids for all physical, chemical and microbial parameters (Clarke 1993). The chemical variables were incorporated into a Non-metric MultiDimensional Scaling (NMDS) ordination plot in order to graphically synthesize the Euclidean dissimilarity between soil samples. Chemical and microbial data were then projected onto the NMDS ordination using a vector-fitting procedure, in which the length of the arrow is proportional to the correlation between NMDS axes and each variable. This method allowed determining the variation pattern of each projected variable discriminating the samples (Foulquier *et al.* 2013; Amalfitano *et al.* 2014). Chemical data were log-transformed, whereas values of microbial groups revealed by NGS (clusters >1% of total OTUs were considered) were normalized by log(X + 1). Shannon and Simpson indices for each sampling site were also generated using PAST software (PALAEON-TOLOGICAL STATISTICS, ver. 2.17) (Hammer, Harper and Ryan 2001).

RESULTS

Physicochemical characteristics of the sampling sites

The variation patterns of major physicochemical parameters differentiated samples in transition from the area not affected by hydrothermal fluids (S4, S5) relative to the most affected ones (S1, S2, S3 and Fangaia mud pools), as revealed by NMDS analysis (Fig. 2).

Sites S1, S2 and S3 were characterized by temperature-depth gradients ≥1.1°C/cm, with soil temperatures at 10 cm depth ranging from 26.3 (S3) to 42.9°C (S2) and from 50.6 (S3) to 60.1°C at 30 cm depth (S2). The pH values ranged from 1.3 to 1.7 at S1 and S2, whereas they were slightly higher (from 2.0 to 2.2) at S3. The ΦCO_2 and ΦCH_4 values ranged from 557 to 3350 and from 0.0021 to 0.059 g m^{-2} day^{-1}, respectively, in agreement with those previously measured at the Solfatara Crater (Cardellini *et al.* 2003; Tassi *et al.* 2013). The chemical composition of the interstitial soil gases was dominated by CO_2 (943 mmol/mol), with relevant concentrations of H_2S and CH_4 (up to 1.9 and 0.091 mmol/mol) and low O_2 content (from 0.32 to 6.1 mmol/mol at 30 cm depth). The $\delta^{13}C$-CO_2 values ranged from -1.86 to -1.1 ‰ vs. V-PDB and increased passing from 30 to 10 cm depth (Table 1). The organic

Table 1. Main physicochemical parameters (T, pH), CO_2 and CH_4 soil fluxes, and chemical and isotopic composition of interstitial soil gases and bubbling gases from the Solfatara Crater. Loss on ignition (L.O.I.) values (in wt%) for soil and mud samples are also reported; n.a.: not analyzed; b.d.l.: below detection limit.

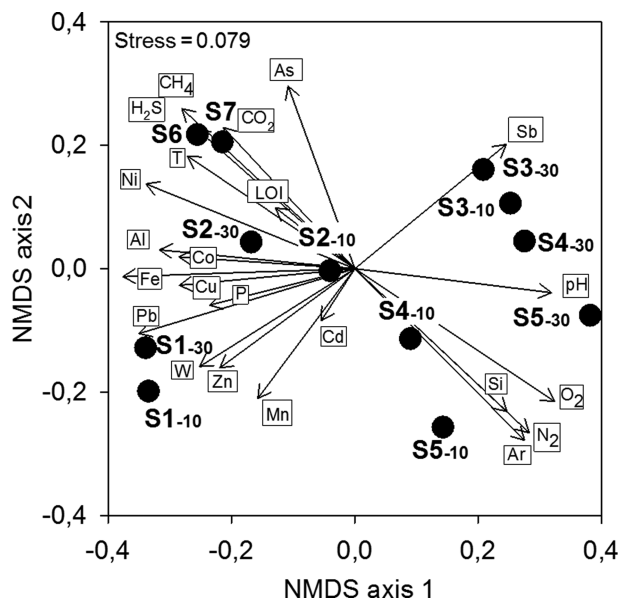| Sample ID	Sampling site	East UTM	North UTM	ϕCO_2 g m^{-2} day^{-1}	ϕCH_4 g m^{-2} day^{-1}	depth cm	T °C	pH -	L.O.I wt%	CO_2 mmol/mol	H_2S mmol/mol	CH_4 mmol/mol	N_2 mmol/mol	O_2 mmol/mol	Ar mmol/mol	H_2 mmol/mol	CO mmol/mol	$\delta^{13}C\text{-}CO_2$ ‰
S1.10	S1	427 588	4 519 913	3350	0.059	10	37.2	1.3	7.3	887	1.6	0.064	109		1.4	b.d.l.	b.d.l.	-1.42
S1.30						30	57.6	1.4	6.2	943	1.9	0.091	54	0.32	0.68	b.d.l.	b.d.l.	-1.69
S2.10	S2	427 539	4 519 923	557	0.0021	10	42.9	1.5	9.9	887	1.3	0.021	107	3.3	1.4	b.d.l.	b.d.l.	-1.1
S2.30						30	60.1	1.7	5.5	900	1.9	0.051	96	0.7	1.3	b.d.l.	b.d.l.	-1.26
S3.10	S3	427 352	4 519 984	896	0.0025	10	26.3	2.2	6.4	804	1.2	0.047	147	46	1.8	b.d.l.	b.d.l.	-1.25
S3.30						30	50.6	2.0	4.8	888	1.6	0.056	103	6.1	1.3	b.d.l.	b.d.l.	-1.86
S4.10	S4	427 571	4 520 048	161	0.00046	10	10.5	2.8	6.5	330	0.31	0.0078	591	71	7.7	b.d.l.	b.d.l.	+0.6
S4.30						30	12.4	3.4	5.8	590	0.56	0.015	390	15	4.8	b.d.l.	b.d.l.	-0.07
S5.10	S5	427 388	4 520 113	110	0.00021	10	14.4	3.4	15	15	0.05	0.0033	733	163	89	b.d.l.	b.d.l.	b.d.l.
S5.30						30	17.4	3.6	8.6	30	0.06	0.0039	741	138	91	b.d.l.	b.d.l.	b.d.l.
S6	Fangaia	427 411	4 519 902	-	-	-	70	2.1	27	987	1.88	0.25	8.45	0.011	0.055	1.85	0.015	n.a.
S7	Fangaia	427 380	4 519 910	-	-	-	40	1.9	21									

Figure 2. NMDS ordination plot, based on Euclidean distance matrix of log-transformed data, showing the variation patterns of chemical variables. The vector length is proportional to the correlation between the NMDS axes and each chemical variable. The stress value (i.e. <0.2) provides an accurate representation of the dissimilarity among areas affected or not affected by hydrothermal fluids.

gases mostly consisted of alkanes (up to 73% ΣVOCs) and aromatics (up to 27% ΣVOCs), whilst cyclic, O-substituted and S-bearing and alkene compounds were ≤4.5, ≤3.2, ≤1.1 and ≤0.30% ΣVOCs, respectively (Table 2).

Soils at S1, S2 and S3 were characterized by L.O.I. values ranging from 4.8 up to 9.9 wt% and relatively high concentrations of SiO_2 (up to 91 wt%), followed by Al_2O_3 (up to 4.5 wt%), S (up to 2.8 wt%), K_2O (up to 2.7 wt%) and TiO_2 (up to 1.35 wt%). Fe_2O_3, CaO, Na_2O, Ba and P_2O_5 were detected at concentrations ranging from 0.10 to 0.48 wt%, whilst Sr, Cl, MgO, Nb, MnO, Pb, Rb, Zr and Cu were ≤0.06 wt%. Cr, As, Y and Hg were only occasionally detected (Table 3). Al, Fe and Si were the most abundant metals measured in the leachates (Table 4). Cu, Mn, Zn, P, As and Pb were present at concentrations ranging from 1.1 to 7.2 mg/L, whilst the contents of W, Ni, Co, Cd and Sb were ≤0.73 mg/L (Table 4).

Relatively highly acidic pH (<2.1) and high temperatures (between 40 and 70°C) were measured for the S6 and S7 muds. The chemical composition of the bubbling gas from the Fangaia mud pools was similar to that of soil gases from sites S1, S2 and S3, i.e. largely dominated by CO_2 (987 mmol/mol) and H_2S (1.88 mmol/mol) (Table 1). Significant H_2 and CH_4 contents (1.85 and 0.25 mmol/mol, respectively), markedly higher than those recorded in soil gases, were measured. Carbon monoxide was also found at a detectable amount (0.015 mmol/mol), whilst O_2 content was 0.011 mmol/mol. The organic gas fraction was largely dominated by ethane and benzene (Table 2). The chemical composition of the water was characterized by high concentrations of SO_4^{2-} (~1800 mg/L) and pH values of 1.62–1.75 (Table 5). Mud samples showed relatively high L.O.I. values (Table 1). The leachates had relatively high concentrations of Al, Fe and Si, as well as of As, Cu and P (Table 4). The concentrations of Mn, Zn, W, Ni, Co, Sb, Pb and Cd were ≤0.52 mg/L.

Sites S4 and S5 displayed soil temperature gradients ≤0.1°C/cm and temperatures ≤17.4°C, whilst the pH values ranged from 2.8 to 3.6 (Table 1). The ΦCO₂ and ΦCH₄ values were ≤161 and ≤0.00046 g m^{-2} day^{-1}, respectively. Interstitial soil

gases were enriched in atmospheric components, i.e. N_2, O_2 and Ar. The CO_2 contents largely differed among these sites, being ≥330 mmol/mol at S4 and ≤30 mmol/mol at S5. Similarly, H_2S and CH_4 concentrations of S4 were higher than those of S5 (Table 1). The δ^{13}C-CO_2 values at S4 were 0.6 and -0.07 ‰ vs. V-PDB at 10 and 30 cm depth, respectively. VOCs were below the detection limit at S5, whereas at S4 they were dominated by alkanes (up to 61% ΣVOCs) and aromatics (up to 24% ΣVOCs) (Table 2). Whilst relative abundances of alkenes (up to 0.20% ΣVOCs) and cyclic compounds (up to 5.01% ΣVOCs) were similar to those of S1, S2 and S3, S-bearing species exhibited lower concentrations (≤0.84% ΣVOCs) and those of O-substituted species were higher (up to 23% ΣVOCs). Soils were characterized by L.O.I. values ranging from 5.8 to 15 wt% (Table 1) and dominated by SiO_2 (up to 86 wt%), followed by Al_2O_3 (up to 5.2 wt%) and K_2O (up to 2.1 wt%). TiO_2 and S were up to 0.95 and 1.2 wt%, whereas Fe_2O_3, CaO, Na_2O, MgO, P_2O_5, Cl and MnO were less than 1.9, 0.72, 0.38, 0.22, 0.21, 0.12 and 0.02 wt%, respectively (Table 3). Ba, Zr, Sr, Pb, Nb, Rb and Cu were present in concentrations ranging from 0.004 to 0.13 wt%, whereas those of Cr and As were below the instrumental detection limit. Ni, Zn and Br were only detected in soils from S5. The chemical composition of leachates showed relatively high concentrations of Al, Fe and Si (Table 4).

Microbial community composition

Overall, CARD-FISH analysis showed that approximately 74.3% of total DAPI-stained cells represented Bacteria and Archaea. On average, 36.6% were Archaea and 37.7% belonged to the Bacteria domain. Abundance of Archaea varied between 6.1 × 10⁶ and 3.2 × 10⁷ cell/g and bacterial cell abundance ranged from 9.4 × 106–4.2 × 10⁷ cell/g (Fig. 3). A total of 1902 856 reads that mapped to Archaea resolved into 43 OTUs. The archaeal 16S rRNA gene fragments resolved into two main phyla: (i) *Euryarchaeota* dominated the S1, S2, S3, S6 and S7 samples (on average 96.5% of total OTUs); and (ii) *Thaumarchaeota* dominated S4 and S5 samples (on average 89.7% of total OTUs). *Crenarchaeota* phylum represented low-abundance taxa only in S2 and S3 deep samples (Fig. 4).

Euryarchaeota phylum was largely represented by the genera *Acidiplasma* (up to 75.8% in S6), *Ferroplasma* (more than 90% in S1–10, and S7 samples) and *Thermoplasma* (on average 91.5% of total OTUs in S3 samples). On average, more than 30% of total OTUs affiliated with the *Thaumarchaeota* terrestrial group in S4 and S5 samples, a large number of OTUs that affiliated with this phylum (up to 96.7% of total OTUs in S4–30), could not be identified at a more specific level, and were described as 'other *Thaumarchaeota*'. *Crenarchaeota* were represented by members affiliated with the *Sulfolobaceae* family, mainly belonging to *Acidianus brierleyi* species.

A total of 2122 238 reads were generated using the bacterial v4v5 primers and they resolved into 921 OTUs. *Proteobacteria* were the most abundant phylum at S1, S2, S3, S6 and S7 (on average 77.5% of total OTUs), with *Gammaproteobacteria* belonging to *Acidithiobacillus* genus ranging from 29.5 to 87.8% of total OTUs. *Alpha-, Beta-* and *Deltaproteobacteria* were mainly retrieved from S2–30 and S3, with relative abundances ranging between 2.5–17.2%, 0.1–2.2% and 0.4–2.3%, respectively.

Firmicutes retrieved in sites S1, S2, S3 and S7 (range 5.8–14.5% of total OTUs) were mainly affiliated with the *Sulfobacillus* (S1, S2 and S3) (range 1.2–10.3%) and *Bacillus* (S2–30) (9.1%). *Actinobacteria* (average 7.1%) were predominantly represented by the *Acidimicrobiales* order and *Mycobacterium* genus. OTUs affiliated

Table 2. Volatile Organic Compounds (VOCs) in interstitial soil gases and bubbling gases from the Solfatara Crater; b.d.l.: below detection limit; n.a.: not analyzed.

Sample ID	nmol/mol													
	C_2H_6	C_3H_8	nC_4H_{10}	iC_4H_{10}	C_6H_6	C_{5+} alkanes	C_3H_6	alkenes	branched aromatics	kenotes	aldehydes	carboxyl acids	cyclics	S-substituted
S1_10	180	60	30	50	130	6.0	b.d.l.	1.4	3.1	3.2	4.1	3.8	15	5.5
S1_30	310	90	50	70	170	11	b.d.l.	1.8	4.5	1.2	2.4	2.6	34	7.8
S2_10	220	90	60	50	150	7.3	b.d.l.	1.6	2.8	4.1	5.5	4.7	21	6.6
S2_30	250	110	80	50	160	9.0	b.d.l.	2.1	3.6	2.6	3.1	3.5	29	7.4
S3_10	250	120	60	80	150	9.0	b.d.l.	1.4	4.8	7.4	9.1	6.9	31	6.1
S3_30	290	150	90	110	180	12	b.d.l.	1.7	6.9	3.7	4.4	3.1	39	7.1
S4_10	50	10	10	0	30	2.0	b.d.l.	0.2	0.7	9.5	16	7.7	4	0.7
S4_30	110	30	20	20	70	4.0	b.d.l.	0.6	2.2	7.8	11	6.1	15	2.5
S5_10	b.d.l.	b.d.l.	b.d.l.	b.d.l.	b.d.l.	b.d.l.	b.d.l.	b.d.l.	b.d.l.	b.d.l.	b.d.l.	b.d.l.	b.d.l.	b.d.l.
S5_30	b.d.l.	b.d.l.	b.d.l.	b.d.l.	b.d.l.	b.d.l.	b.d.l.	b.d.l.	b.d.l.	b.d.l.	b.d.l.	b.d.l.	b.d.l.	b.d.l.
S6	1900	12	11	6.1	850	n.a.	0.9	n.a.	n.a.	n.a.	n.a.	n.a.	n.a.	n.a.
S7														

to *Thermotogae* phylum were retrieved at relatively low abundances in all samples (<0.1%) with the exception of sample S6 where they represented 40.9% of total OTUs. Members of *Nitrospirae* phylum that primarily affiliated with *Leptospirillum* genus represented 5.6% and 1.9% of total OTUs in S3-10 and S3-30 samples, respectively (Fig. 5).

Remarkably, sites S4 and S5 harbored completely different bacterial community compositions. The Shannon index showed the highest values in these samples (range between 1.9 and 3.7) and the lowest ones in all other samples (on average 1.2). Similar trends were also found using the Simpson index showing values on average equal to 0.4 in all samples, with the exception of S4 and S5 samples (index values ≥0.8). In S4 and S5 samples the main phyla retrieved were *Acidobacteria* (36.7% of total OTUs), *Chloroflexi* (25.7%), *Proteobacteria* (14.1%), *Actinobacteria* (5.7%), *Firmicutes* (4.1%), *Bacteroidetes* (2.9%), *Planctomycetes* (2.7%) and *Verrucomicrobia* (1.1%). Between 4% and 12% of bacterial OTUs were not identified at the phylum level in S4 samples by GAST (see 'other bacteria' in Fig. 5). The majority of these 'bacterial' OTUs (up to 99%) showed high sequence identity to *Nitrososphaera* and 'Candidatus Parvarchaeum' when the sequences were queried against the full NCBI nucleotide database (Altschul *et al.* 1990, 1997) and the RDP classifier database (Wang *et al.* 2007). *Acidobacteria* were affiliated with *Acidobacteriales* order and *Bryobacter* genus, although a large amount (up to 39.3% in S4–10) was not identified at genus level. *Chloroflexi* were mainly affiliated with *Ktedonobacterales* order (up to 53% in S4–30), mostly belonging to *Ktedonobacteraceae* and *Thermosporotrichaceae* families. *Proteobacteria* showed the highest percentage in S5 (up to 25%), represented by *Alpha-* (*Rhodospirillales*), *Beta-* (*Neisseriales*) and *Gammaproteobacteria* (*Haemophilus* genus). OTUs affiliated to *Streptococcus* genus, belonging to *Firmicutes* phylum, represented more than 11% of total OTUs in S5–10 (Fig. 5).

DISCUSSION

Geochemical features

The selected sites showed a wide range of environmental conditions, in terms of temperature, pH, and supply of hydrothermal fluids. The latter can roughly be estimated from the measurements of CO_2 diffuse fluxes from the Solfatara Crater floor. Among the measuring sites, the highest ΦCO_2 values were

measured at S1, S2 and S3, where temperatures ranged from mesophilic (at 10 cm depth) to thermophilic (at 30 cm depth) values. Similarly, the ΦCH_4 values were up to two orders of magnitude higher than those measured in sites S4 and S5, suggesting a strong contribution of hydrothermally derived fluids. Accordingly, the chemical composition of interstitial soil gases collected at both 10 and 30 cm depths in sites S1, S2 and S3 approached that of the fumarolic gas emissions, being dominated by CO_2 and characterized by relatively high contents of H_2S and CH_4, as well as ethane, benzene, alkenes and S-bearing compounds. The isotopic composition of CO_2 in the interstitial soil gases from S1, S2 and S3 (from -1.86 to -1.1 ‰ vs. V-PDB) was consistent with that reported for the fumarolic emissions from the Solfatara (i.e. from -2 to -0.95 ‰ vs. V-PDB; Chiodini *et al.* 2008; Vaselli *et al.* 2011; Tassi *et al.* 2015a), confirming a dominating hydrothermal fluid input. The strong uprising of hydrothermal fluids was responsible for the peculiarly acidic conditions (pH ≤ 2.2) measured in these sites, since H_2S is rapidly oxidized, either abiotically or biotically, under aerobic conditions to form sulfuric acid that affects minerals producing whitish deposits, as those recognized on the Solfatara Crater floor and at S1, S2 and S3 (Fig. 1). When compared to the parent material (Turney *et al.* 2008 and references therein), the analyzed soil samples were enriched in immobile elements, such as Ti and Si (Fig. 6a), and depleted in mobile species, i.e. Na, Ca, K and Mg (Fig. 6a), as well as Mn and Cl (Fig. 6b), testifying intense alteration processes. The depletion in Al and Fe observed in the soil samples with respect to volcanic rocks was related to the acidic conditions, which increase the mobility of these metals during leaching processes. The relatively high S concentrations (up to 2.79 wt%), e.g. those measured in S1, S2 and S3, confirmed the strong interaction with hydrothermal H_2S-rich fluids. Relatively high concentrations of Al, Fe, Cu, Mn, Zn, P, Pb, W, Cd, Co and Ni were measured in the leachates from S1, S2 and S3 soil samples (Table 4), suggesting that these metals were available for uptake due to the low-pH conditions. Similarly, the S6 and S7 samples were characterized by a relatively high mobility of metals such as Fe, Al, Cu, P, Sb, Co, Ni and, particularly, As, which reached concentrations ~3 mg/L in the leachates. The occurrence of such peculiar high concentrations of metals in the Fangaia muds was likely caused by an enhanced hydrothermal fluid contribution. Waters

Table 3. Bulk chemical composition (expressed in wt%) resulting from XRF analysis on soil samples; b.d.l.: below detection limit; n.a.: not analyzed.

Sample ID	wt%																									
	Na$_2$O	MgO	Al$_2$O$_3$	SiO$_2$	P$_2$O$_5$	K$_2$O	CaO	TiO$_2$	MnO	Fe$_2$O$_3$	S	Cl	Cu	Rb	Sr	Zr	Nb	Ba	Pb	Cr	As	Y	Hg	Ni	Zn	Br
S1.10	0.19	0.040	4.5	81	0.099	2.7	0.24	0.99	b.d.l.	0.48	2.6	0.020	0.004	0.016	0.057	0.046	0.008	0.13	0.009	0.009	b.d.l.	b.d.l.	b.d.l.	b.d.l.	b.d.l.	b.d.l.
S1.30	n.a.	n.a.	n.a.	n.a.	n.a.	n.a.	n.a.	n.a.	n.a.	n.a.	n.a.	n.a.	n.a.	n.a.	n.a.	n.a.	n.a.	n.a.	n.a.	n.a.	n.a.	n.a.	n.a.	n.a.	n.a.	n.a.
S2.10	0.046	0.016	1.6	83	0.061	0.53	0.071	1.1	b.d.l.	0.19	2.8	0.022	0.004	0.004	0.011	0.054	0.009	0.14	0.013	0.013	b.d.l.	b.d.l.	b.d.l.	b.d.l.	b.d.l.	b.d.l.
S2.30	0.064	0.021	1.4	89	0.060	0.44	0.080	1.2	b.d.l.	0.19	1.5	0.050	0.006	0.004	0.010	0.062	0.011	0.15	0.008	b.d.l.	0.012	0.000	b.d.l.	b.d.l.	b.d.l.	b.d.l.
S3.10	0.065	0.024	3.2	86	0.10	0.98	0.070	1.1	b.d.l.	0.18	1.3	0.040	b.d.l.	0.004	0.012	0.083	0.015	0.12	0.015	b.d.l.	b.d.l.	b.d.l.	0.006	b.d.l.	b.d.l.	b.d.l.
S3.30	0.028	0.022	1.1	91	0.10	0.17	0.070	1.4	0.009	0.11	0.65	0.030	b.d.l.	0.003	0.006	0.098	0.017	0.12	0.018	b.d.l.	b.d.l.	0.009	0.009	b.d.l.	b.d.l.	b.d.l.
S4.10	0.12	0.050	3.2	85	0.12	1.4	0.23	0.89	0.010	0.96	0.89	0.12	0.005	0.006	0.019	0.048	0.008	0.12	0.018	b.d.l.	b.d.l.	0.000	b.d.l.	b.d.l.	b.d.l.	b.d.l.
S4.30	0.12	0.050	3.5	86	0.099	1.5	0.15	0.62	b.d.l.	0.45	1.2	0.039	0.004	0.007	0.019	0.052	0.009	0.11	0.012	b.d.l.	b.d.l.	b.d.l.	b.d.l.	b.d.l.	b.d.l.	b.d.l.
S5.10	0.38	0.22	5.2	72	0.21	2.1	0.72	0.80	0.020	1.9	1.0	0.080	0.005	0.010	0.026	0.059	0.009	0.13	0.023	b.d.l.	b.d.l.	b.d.l.	b.d.l.	0.008	0.015	0.002
S5.30	0.25	0.11	3.9	82	0.12	1.9	0.43	0.95	0.010	0.94	0.79	0.059	0.004	0.009	0.023	0.058	0.011	0.13	0.020	b.d.l.	b.d.l.	b.d.l.	b.d.l.	0.003	0.004	0.002
S6	n.a.	n.a.	n.a.	n.a.	n.a.	n.a.	n.a.	n.a.	n.a.	n.a.	n.a.	n.a.	n.a.	n.a.	n.a.	n.a.	n.a.	n.a.	n.a.	n.a.	n.a.	n.a.	n.a.	n.a.	n.a.	n.a.
S7	n.a.	n.a.	n.a.	n.a.	n.a.	n.a.	n.a.	n.a.	n.a.	n.a.	n.a.	n.a.	n.a.	n.a.	n.a.	n.a.	n.a.	n.a.	n.a.	n.a.	n.a.	n.a.	n.a.	n.a.	n.a.	n.a.

Table 4. Chemical composition resulting from ICP-OES analysis of solutions obtained after leaching tests in MilliQ on soil and mud samples; b.d.l.: below detection limit.

Sample ID	mg/L														
	Mn	Fe	Co	Ni	Cu	Zn	As	Sb	Al	Hg	W	Si	Pb	P	Cd
S1_10	3.7	488	0.17	0.11	2.4	1.2	0.17	b.d.l.	1110	b.d.l.	0.73	47	1.09	1.6	0.03
S1_30	2.8	229	0.16	0.18	5.0	1.9	0.15	b.d.l.	873	b.d.l.	0.59	93	0.15	0.83	0.11
S2_10	0.62	13	0.03	0.04	0.59	0.48	0.55	0.04	278	b.d.l.	0.54	24	0.06	0.75	0.03
S2_30	1.0	59	0.11	0.15	7.2	0.9	1.4	0.04	273	b.d.l.	0.48	24	0.61	0.51	0.05
S3_10	0.67	8.7	0.04	0.04	0.17	0.41	0.35	0.04	107	b.d.l.	0.44	79	b.d.l.	0.63	0.03
S3_30	1.0	10	0.03	0.05	0.94	0.69	0.55	0.07	157	b.d.l.	0.43	71	b.d.l.	0.48	0.04
S4_10	0.82	19	0.04	0.04	0.21	0.46	0.21	0.03	15	b.d.l.	0.40	96	0.01	0.42	0.04
S4_30	0.72	8.4	0.04	0.04	0.18	0.34	0.17	0.04	24	b.d.l.	0.39	91	b.d.l.	0.27	0.03
S5_10	0.60	5.9	0.02	0.04	0.29	0.48	0.27	0.06	23	b.d.l.	0.40	125	0.08	1.4	0.03
S5_30	1.1	4.0	0.02	0.04	0.28	0.64	0.48	0.08	10	b.d.l.	0.40	114	b.d.l.	0.66	0.07
S6	0.50	133	0.27	0.28	1.8	0.51	3.7	0.12	139	b.d.l.	0.41	18	0.13	1.2	0.04
S7	0.52	53	0.02	0.20	0.22	0.37	2.9	0.03	133	b.d.l.	0.41	24	0.14	1.6	0.03

Table 5. Main physicochemical parameters (Eh and pH) and chemical composition of water from Fangaia mud pools; b.d.l.: below detection limit.

Sample ID	pH	Eh	F	Cl	Br	NO	SO^2	Ca^2	Mg^2	Na	K	NH	Li
	-	mV	mg/L	mg/L	mg/L	mg/L	mg/L	mg/L	mg/L	mg/L	mg/L	mg/L	mg/L
S6	1.62	447	5.30	101	b.d.l.	4.36	1810	20	2.45	80	47	b.d.l.	b.d.l.
S7	1.75	388	2.77	95	b.d.l.	0.78	1800	11	b.d.l.	5.31	14	b.d.l.	1.33

collected from S6 and S7 displayed temperatures in the thermophilic range and a typical sulfate-acidic composition, which was likely produced by the condensation of hydrothermal fluids into near-surface groundwater. The relatively high CH_4 and H_2 concentrations in the bubbling gas from Fangaia mud pools with respect to those measured in the fumarolic vents may be related to a higher contribution of reduced hydrothermal fluids. The markedly high concentrations of ethane and benzene in the Fangaia gases support this hypothesis.

In contrast, S5 was characterized by N_2-dominated interstitial soil gas compositions and relatively high O_2 contents (≥ 138 mmol/mol), corresponding to the lowest ΦCO_2 and ΦCH_4 values, pointing to a low supply of hydrothermal fluids. This was confirmed by both psychrophilic soil temperatures and relatively high pH values. The 10 and 30 cm samples from S5 showed relatively high concentrations of metals with respect to those recorded in other soil samples but they were depleted relative to the parent volcanic rocks. This implies a less intense hydrothermal alteration process with respect to the other sampling sites. The higher pH values produced the observed lower mobility of metals, except for P, the latter being enriched in S5 at 10 cm depth with respect to the P content measured in the parent material. Such enrichment likely reflects the decomposition of organic matter. Accordingly, S5 was located in a portion of the crater covered by luxuriant vegetation, i.e. a typical mesophilic Mediterranean forest (Fig. 1). A circumscribed vegetation cover was also present at S4, which was totally enclosed among hydrothermalized terrains (Fig. 1). Here, CO_2 was the most abundant gas species at 30 cm depth, where increased concentrations of H_2S, CH_4, ethane, benzene, alkenes and S-bearing organic compounds from the hydrothermal source were also measured.
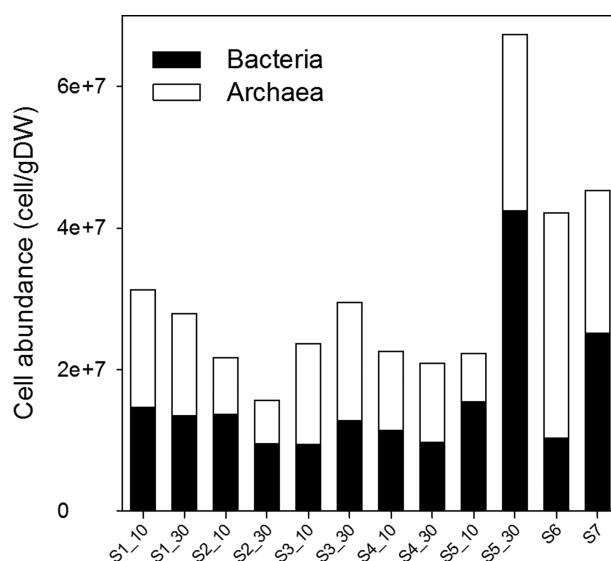
Figure 3. Bacteria and Archaea abundance estimated by CARD-FISH and expressed as number of cells per gram of dry weight (DW). Cells were hybridized by the specific probes EUB338 I-III and ARCH915 for Bacteria and Archaea, respectively.

Hints of possible biochemical processes affecting C-bearing species in soil gases

The correlation among (i) CO_2, CH_4 and H_2S contents, (ii) high temperatures, (iii) acidic conditions, and (iv) CO_2 and CH_4 fluxes clearly indicates a hydrothermal origin for both CO_2 and CH_4 in the interstitial soil gases from the analyzed sites throughout the Solfatara Crater. A dominant deep CO_2-rich source was
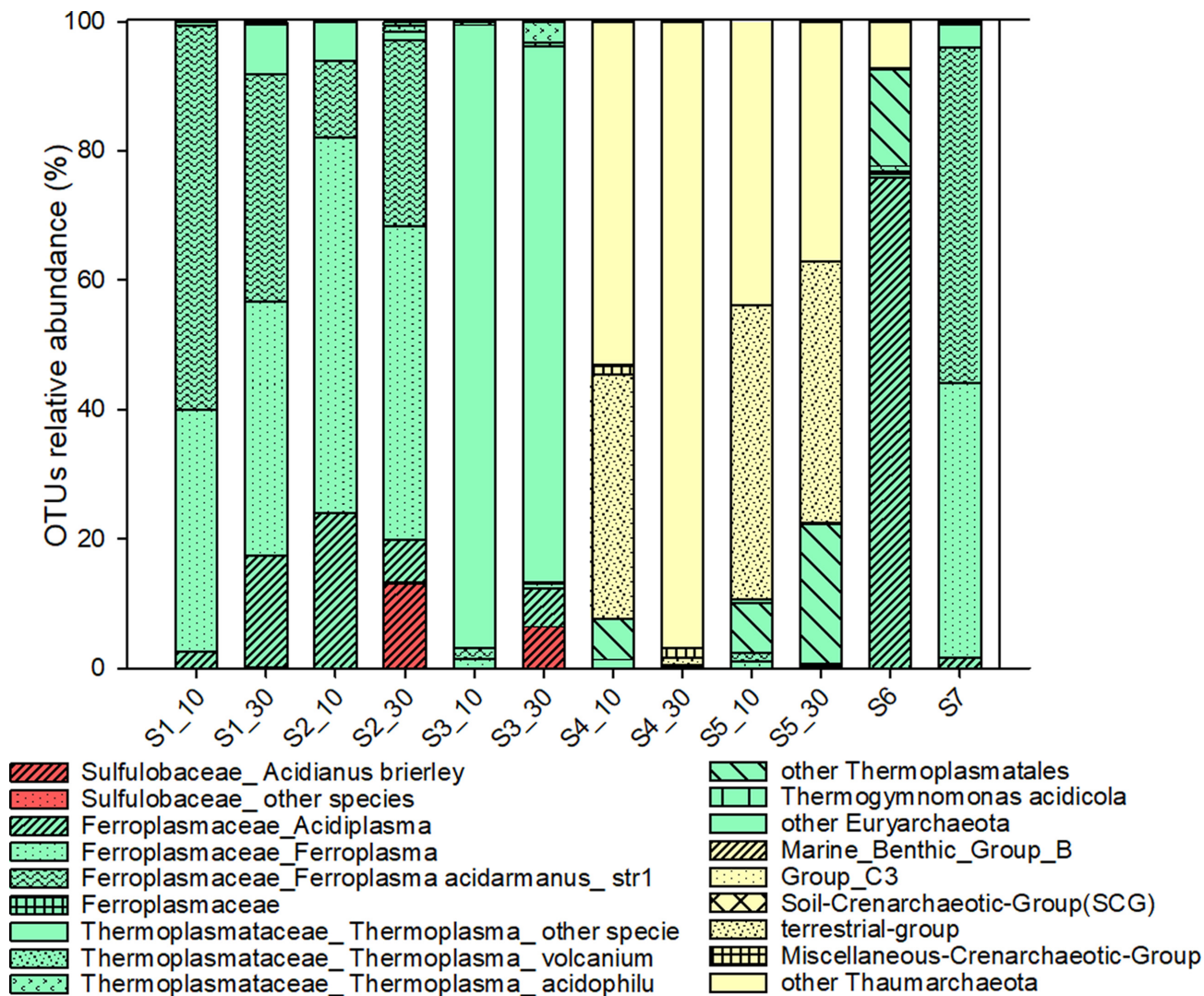
Figure 4. Relative abundance (% of total OTUs) of OTUs belonging to the domain of Archaea estimated by NGS. Crenarchaeota (red); Euryarchaeota (green); Thaumarchaeota (yellow).

confirmed by the carbon isotopic composition in S1 soil gases, which resembled that of the fumarolic emissions. Moving from S1 to S4, the isotopic composition of CO_2 progressively diverged from that of the fumarolic discharges, increasing up to 0.6 ‰ vs. V-PDB in S4 at 10 cm depth. Despite the progressive depletion in CO_2 and enrichment in atmospheric gases (N_2, O_2, Ar) suggesting the occurrence of a certain air dilution, a mixing of hydrothermally derived CO_2 with air (δ^{13}C-CO_2 value around -8 ‰ vs. V-PDB) would lead to a progressive decrease in δ^{13}C-CO_2 values. Hence, a simple dilution process cannot explain the observed geochemical features. Hence, fractionation processes able to modify the isotopic signature of hydrothermal CO_2 were likely occurring. The increase of the δ^{13}C-CO_2 values from 30 cm to 10 cm depth at S1, S2, S3 and S4 is consistent with the occurrence of isotopic fractionation processes affecting the deep-sourced CO_2 in the shallowest portions of the system. According to Federico et al. (2010), the carbon isotopic composition of interstitial soil gases is expected to be controlled by fractionation effects during the CO_2 uprising through the soil. However, no clear relationship between δ^{13}C-CO_2 variations from 30 to 10 cm depth and ΦCO_2 values were observed (Table 1). On the other hand, the relative enrichment in $^{13}CO_2$ observed in the soil

gases at decreasing CO_2 contents could be related to biochemical processes. Autotrophic CO_2 fixation preferentially consumes the isotopically light CO_2, causing a ^{13}C enrichment in residual soil CO_2 compatible with the observed increasing trend in δ^{13}C-CO_2 values at decreasing CO_2 contents in soil gases (Table 1).

The CO_2/CH_4 ratio in the soil gases increased from S1 to S4, suggesting that deep-sourced CH_4 was consumed more efficiently than CO_2 at decreasing hydrothermal fluid inputs. Although CH_4 can be considered almost chemically inert, the presence of specific inorganic catalysts (minerals, metals) or the enzymatic activity of methanotrophs may allow either abiotic or biotic oxidation of CH_4, respectively. The increase of the CO_2/CH_4 ratio from 30 cm to 10 cm depth at S1 to S4 suggests a significant consumption of deep-sourced CH_4 at shallow depths in the soil. Particularly favorable conditions for the development of CH_4 consumption processes seem to characterize S4 and S2 at 10 cm depth. In contrast, the peculiarly low CO_2/CH_4 ratio at S5 indicates prevailing CO_2 consumption processes over CH_4 oxidation. The CO_2 content in the S5 soil declined by 50% between 30 cm and 10 cm depths.

As observed for CO_2 and CH_4, evidence of shallow secondary processes affecting the hydrothermal fluids during their
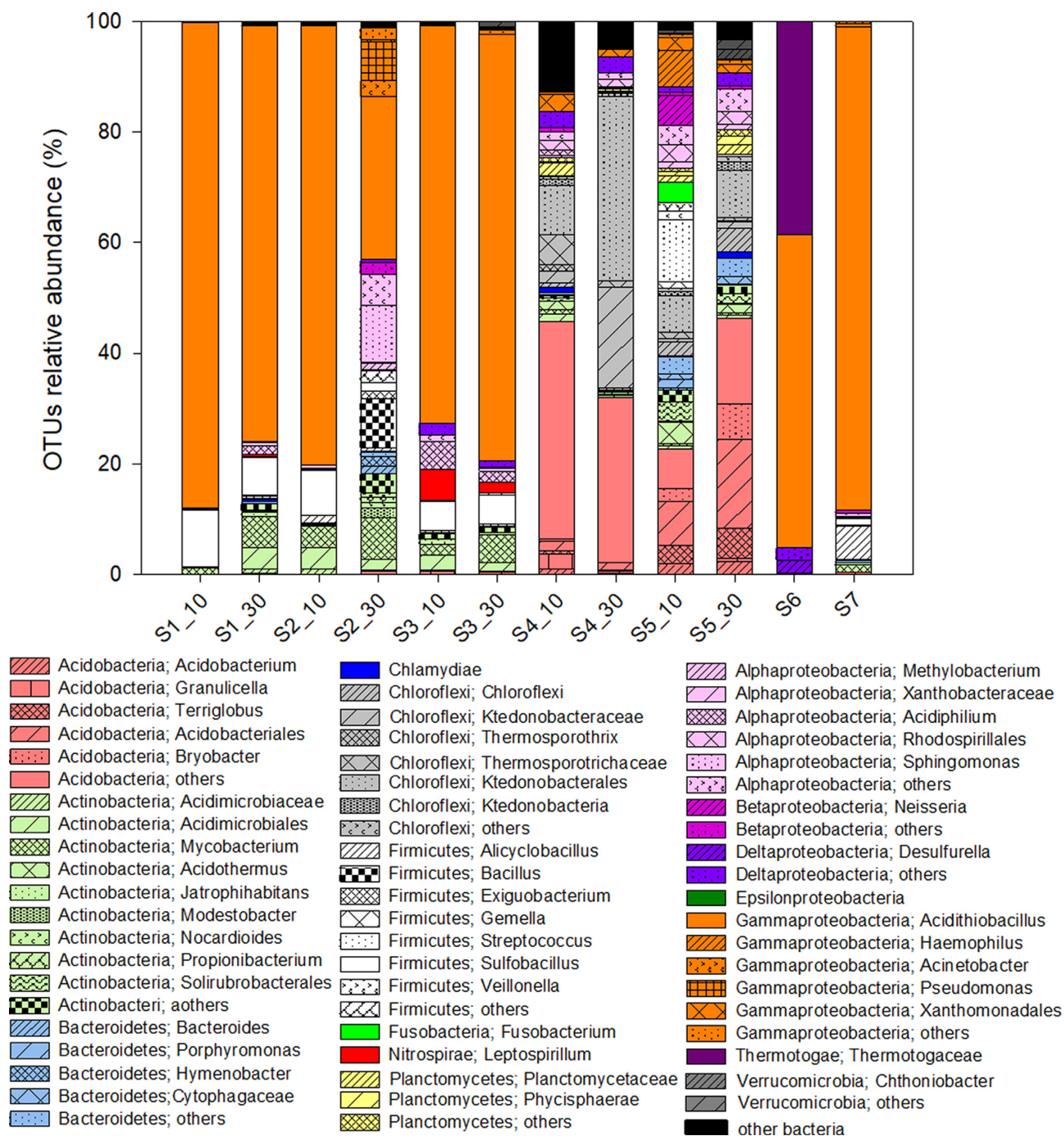
Figure 5. Relative abundance (% of total OTUs) of OTUs belonging to the domain of Bacteria estimated by NGS. Clusters making up less than 1% of total composition and bacteria not identified at phylum level were classified as 'other bacteria'.

migration through the soil towards the atmosphere can also be recognized among VOCs. Hydrocarbons (alkanes, aromatics and alkenes) and S-bearing compounds were detected at higher concentrations in soil gases from S1, S2 and S3 with respect to S4 (Table 2). Their contents in soil gases decreased from 30 cm to 10 cm depth at each sampling site, pointing to a deep origin of these compounds. Accordingly, alkanes, aromatics, alkenes and S-bearing species were recognized as the major organic constituents in fumarolic gases from the Solfatara Crater (Tassi et al. 2015a). Similarly, cyclics showed higher amounts in soil gases from (i) S1, S2 and S3 with respect to

S4, and (ii) at 30 cm depth relative to 10 cm depth in each site. The production of cyclics is thought to occur at relatively great depth through incomplete aromatization of alkanes at temperature <150°C (Tassi et al., 2012, 2015a; Venturi et al. 2017b). The O-bearing compounds (e.g. aldehydes, ketones and carboxylic acids) showed an opposite trend, since increasing concentrations passing from S1, S2 and S3 to S4, and from 30 cm to 10 cm depth, were measured. This was likely due to increasing oxidizing conditions related to the availability of free O_2, being the O-bearing compounds typical by-products of metabolic
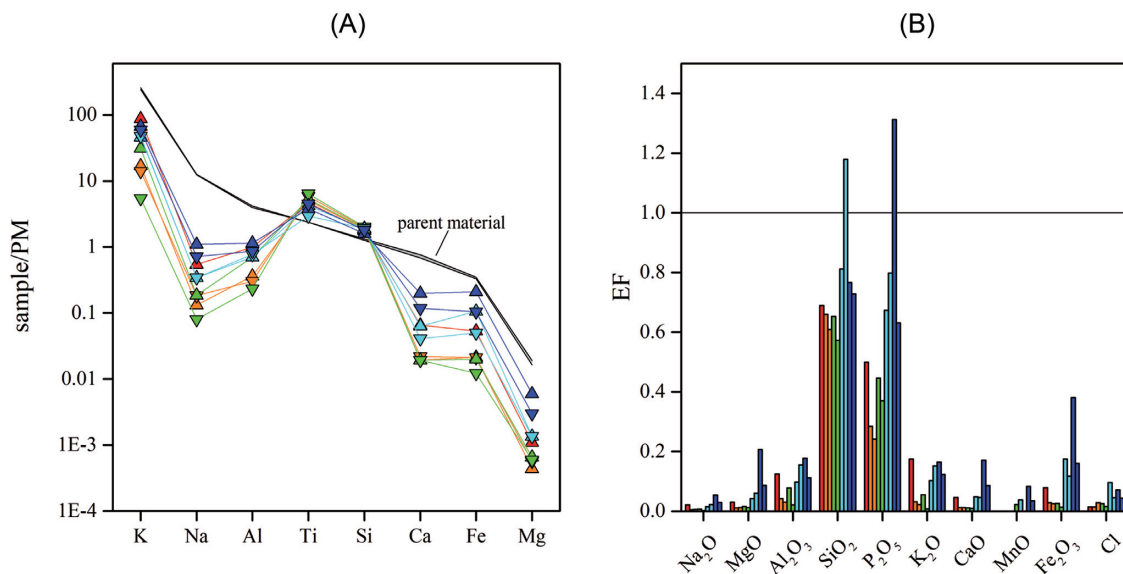
Figure 6. (A) Primitive mantle (PM)-normalized element patterns for soil samples collected at 10 cm (up triangle) and 30 cm (down triangle) depth from sites S1 (red color), S2 (orange color), S3 (green color), S4 (cyan color) and S5 (blue color). The PM-normalized concentrations of parent materials, i.e Solfatara and Astroni trachytes and Agnano Monte Spina phono-trachytes (according to Turney *et al*. 2008 and references therein), are also reported (gray shaded area). **(B)** Enrichment factors (EF) for selected elements relative to parent materials in soil samples from sites S1 (red color), S2 (orange color), S3 (green color), S4 (cyan color) and S5 (blue color) collected at 10 cm (first bar) and 30 cm (second bar) depth. EF values were calculated for each element as follows: $EF_i = \frac{(C_i/C_{TiO_2})_{sample}}{(C_i/C_{TiO_2})_{parent}}$, where $(C_i/C_{TiO_2})_{sample}$ and $(C_i/C_{TiO_2})_{parent}$ are the concentration ratios of an element i normalized to TiO_2 in the sample and in the parent material, respectively.
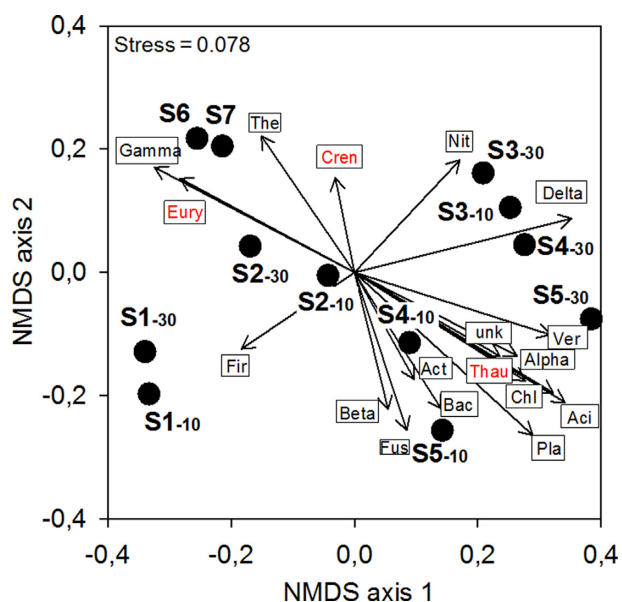
Figure 7. The typifying microbial composition revealed by NGS (clusters >1% of total OTUs were considered) projected onto the NMDS ordination synthesizing the chemical dissimilarity between areas affected or not affected by hydrothermal fluids (see Fig. 2). The vector length is proportional to the correlation between the NMDS axes and each microbial variable, upon normalization by log(X + 1). Bacteria: Aci, Acidobacteria; Act, Actinobacteria; Bac, Bacteroidetes; Chl, Chloroflexi; Fir, Firmicutes; Fus, Fusobacteria; Nit, Nitrospirae; Pla, Planctomycetes; Alpha-, Beta-, Gamma-, Deltaproteobacteria; The, Thermotogae; unk, bacteria unknown. Archaea (in red): Cren, Crenarchaeota; Eury, Euryarchaeota; Thau, Thaumarchaeota.

pathways of microorganisms. For instance, ketones and aldehydes may result from the consumption of alkanes under aerobic conditions (e.g. Fritsche and Hofrichter 2008; Rojo 2009). At S1, S2 and S3, the $C_{5+}/C_{\leq 4}$ alkanes ratio in soil gases decreased

approaching the surface, suggesting the occurrence of efficient consumption of long-chain alkanes at shallow depth. Differently, C_{5+} alkanes were enriched in the S4 soil gases, whose $C_{5+}/C_{\leq 4}$ alkanes ratio increased approaching the soil-air interface, pointing to a shallow source of long-chain saturated hydrocarbons. The latter might be represented by the degradation of organic matter since, differently with respect to what was observed at S1, S2 and S3, a vegetation cover was present at site S4.

Microbiological features

Due to its extreme and harsh conditions, some investigators regard the Solfatara as a plausible terrestrial analogue for Martian hydrothermal systems where physicochemical conditions might be comparable to those of the Archaean Earth (e.g. Glamoclija *et al*. 2004a; Glamoclija, Garrel and López-Garcia 2004b; Glamoclija, Garrel and López-Garcia 2004c; Sgavetti *et al*. 2009). Previous microbiological studies (Huber, Huber and Stetter 2000) recognized the Solfatara Crater, together with Yellowstone National Park (USA), as model systems for studying thermophilic and hyperthermophilic microorganisms in hydrothermal environments. Hot springs, mud holes and Solfataric fields are natural biotopes of thermophilic and hyperthermophilic microorganisms due to their extreme chemical-physical characteristics. Other than the Solfatara and Yellowstone, the most studied hydrothermal environments worldwide are those located in the Kamchatka Peninsula (Russia), the Taupō Volcanic Zone (New Zealand) and Krisuvik, Hveragerthi and Kerlingarfjöll (Iceland) (Huber, Huber and Stetter 2000). A comparison of the biodiversity and community composition in high-temperature, acidic, sulfur-rich sites outlined common microbiological features driven by extreme environmental characteristics. In particular, members belonging to *Sulfolobus*, *Acidithiobacillus* and *Hydrogenobaculum* were frequently recovered (Kvist, Ahring and Westermann 2007; Mathur *et al*. 2007; Inskeep *et al*. 2010, 2013;

Lin *et al.* 2015; Colman *et al.* 2018). At a lower extent, members of *Sulfurihydrogenibium*, *Nanoarchaeum* (Inskeep *et al.* 2010, 2013; Hou *et al.* 2013; Sahm *et al.* 2013; Menzel *et al.* 2015) and *Acidianus* genera were also observed (Stout *et al.* 2009; Menzel *et al.* 2015).

This study provides the first detailed description of microbial communities from the Solfatara soils and sediments using high-throughput sequencing and *in-situ* quantification of Archaea and Bacteria. Overall, CARD-FISH analysis showed a nearly equal occurrence of archaeal and bacterial cells in all screened samples with cell densities (up to 3.2×10^7 and 4.2×10^7 cell/g for Archaea and Bacteria, respectively – Fig. 3) in the range of those observed in previous studies in analogous environments (Huber, Huber and Stetter 2000; Inskeep *et al.* 2010). The sequencing data analysis clearly showed the strong influence of the Solfatara physicochemical characteristics on the structure and composition of the mixed microbial communities. A marked distinction in the microbial composition from the different communities between sites highly affected by hydrothermal fluids (S1-S2-S3-S6-S7) and sites characterized by lower temperatures and higher O_2 concentrations (S4-S5) (Fig. 7) was recorded. Low levels of archaeal and bacterial biodiversity and equitability were found in S1, S2, S3, S6 and S7, typically characterized by elevated temperatures and very low pH values. Higher bacterial biodiversity and concomitant distinctive structure of the archaeal community were observed in S4 and S5 characterized by lower temperatures ($<17.4°C$) and slightly higher pH values (pH = 2.8–3.6). Consistent with the extremely acidic conditions and the high concentrations of metal observed in S1-S2-S3-S6-S7, most of the OTUs retrieved in Archaea domain were affiliated with acidophilic members of family *Ferroplasmaceae*. *Ferroplasma* were found in environments characterized by high temperatures ($>50°C$), suggesting the possibility of the existence of thermophilic members of this genus (Urbieta *et al.* 2012; Menzel *et al.* 2015). At the species level, the analysis revealed the occurrence of '*Ferroplasma acidarmanus*', a facultative anaerobe previously observed in acidophilic hot environments with a temperature of ~40°C (Edwards *et al.* 2000; Aliaga-Goltsman *et al.* 2015). This microorganism is able to grow at pH ranging between 0 and 1.5 either chemoorganotrophically or chemomixotrophically on Fe(II) and a variety of carbon sources (yeast extract, casaminoacids and sugars) (Dopson *et al.* 2004). It can also proliferate, although at low growth rate, by coupling oxidation of organic carbon sources to Fe(III) reduction (Dopson *et al.* 2004).

The prevalence of *Acidiplasma* spp., facultatively anaerobic, acidophilic and thermophilic archaea able to oxidize and reduce iron, was specifically found in S6, which is characterized by the highest temperature registered among the screened sampling sites (70°C) (Golyshina *et al.* 2009). As often observed in acidic Solfataric environments (Segerer *et al.* 1986; Benson *et al.* 2011), the acidic hot and oxygen-exposed surface of terrestrial fields typically harbor aerobic or facultative aerobic archaea such as *Acidianus brierley* found in S2 and S3 samples at lower abundance relative to *Ferroplasma*. The occurrence of Archaea capable of oxidizing sulfur and inorganic sulfur compounds is in line with the biotic H_2S oxidation observed in S2 and S3.

Furthermore, in metal-rich samples (S1-S2-S3-S6-S7) with particularly high As concentrations, the analysis revealed the occurrence of microorganisms potentially involved in arsenic detoxification and metabolic reactions, such as members of genera *Acidiplasma*, *Ferroplasma* and *Thermoplasma* (Baker-Austin *et al.* 2007; Volant *et al.* 2012; Yelton *et al.* 2013). Arsenic is one of the most prominent heavy metals in high-temperature environments, reflecting the occurrence of thermophilic As-transforming microorganisms (Huber, Huber and Stetter 2000;

Hug *et al.* 2014; Wheaton *et al.* 2015). The possible involvement of hyperthermophiles in the As-cycle from these environments is consistent with the previously reported occurrence of arsenate-reducing prokaryotes in Pisciarelli Solfatara and the isolation of *Pyrobaculum arsenaticum* (Huber, Huber and Stetter 2000). Members of *Thermoplasmata* class could also be involved in anaerobic methane oxidation, as frequently observed in sediments (Inagaki *et al.* 2006; Roalkvam *et al.* 2011; Avrahamov *et al.* 2014).

Completely different archaeal communities were observed in S4 and S5 (Fig. 7). These sites were characterized by both relatively higher pH values, lower temperatures, lower H_2S and higher O_2 and N_2 concentrations relative to those sites strongly affected by the presence of hydrothermal fluids. The large majority of OTUs was affiliated with *Thaumarchaeota*, a deep-branching phylum within Archaea domain. Members of this phylum represent the most abundant Archaea on Earth and include all known autotrophic archaeal ammonia oxidizers as well as environmental sequences representing microorganisms with unknown metabolisms (Stieglmeier, Alves and Schleper 2014). However, comprehensive information about energy metabolisms of *Thaumarchaeota* is still lacking. Thus, the involvement of members of this phylum in methane oxidation cannot be excluded. It is well known that ammonia monooxygenase and methane monooxygenase enzymes are evolutionarily linked (Holmes *et al.* 1995), leading to functional similarities enabling both methanotrophy and ammonia oxidation (O'Neill and Wilkinson 1977; Jones and Morita 1983; Zheng *et al.* 2014). Only a few OTUs affiliated with archaeal groups that typically include methanogens (e.g. orders *Methanobacteriales*, *Methanomicrobiales* and *Methanosarcinales*) were detected by the sequencing analysis thus likely indicating a marginal contribution of methanogenesis to the overall metabolic traits of the microbial communities living in this environment.

Among bacteria, most of the OTUs retrieved from S1, S2, S3, S6 and S7 samples belonged to *Acidithiobacillus* genus, which includes acidophilic aerobic bacteria able to autotrophically grow on iron and/or sulfur compounds (Dopson and Johnson 2012). In addition, some strains of *Acidithiobacillus* genus are able to grow under anaerobic conditions via Fe^{3+} respiration, using elemental sulfur, tetrathionate or hydrogen as electron donors (Hedrich and Johnson 2013). Members of this genus were previously observed at Campi Flegrei and in other acidophilic hot hydrothermal springs, rivers and pools worldwide (Urbieta *et al.* 2012; Sahm *et al.* 2013; Wemheuer *et al.* 2013; Menzel *et al.* 2015). It is well known that *Acidithiobacillus* spp. also plays a key role in biofilm formation and sulfur oxidation in extremely acidic environments (Jones *et al.* 2012; Quatrini and Jonson 2018). Together with *Acidithiobacillus*, the occurrence of sequences affiliated with *Sulfobacillus* and *Alicyclobacillus* genera, previously observed in the Pozzuoli area and in other hydrothermal vents (Menzel *et al.* 2015; Guo *et al.* 2016), indicates the presence of a microbial community involved in the biotic H_2S oxidation observed in sites S1, S2 and S3. The analysis also revealed the marginal occurrence of OTUs affiliated to *Leptospirillum* genus (Rawlings, Tributsch and Hansford 1999; Hippe 2000) and *Acidimicrobiales* order (Stackebrandt, Rainey and Ward-Rainey 1997), typically found in acidic metal-contaminated environments and capable of Fe^{2+}-oxidation (Clum *et al.* 2009; Christel *et al.* 2017). Furthermore, the sequencing analysis highlighted the presence of thermophilic methanol consumers belonging to genus *Methylobacterium* in S2 at 30 cm depth. OTUs affiliated with the phylum *Thermotogae* were abundant in S6, which had the highest temperatures and L.O.I. values, in agreement with the results of studies carried out in sites having similar temperatures and pH conditions (Sahm

et al. 2013; Wemheuer *et al.* 2013; Li *et al.* 2015; Menzel *et al.* 2015). As observed for Archaea, the bacterial communities in S4 and S5 exhibited a diversity that was remarkably higher than that found in the other sites. Most OTUs retrieved in these samples were affiliated with the phylum *Acidobacteria* but they exhibited weak relationships to described species. Members of the phylum *Acidobacteria* represent one of the most abundant bacterial groups in soil environments (Jones *et al.* 2009; Foesel *et al.* 2014), but their ecological roles are poorly understood, likely due to a paucity of cultured representatives (Kielak *et al.* 2016). *Acidobacteria* were profusely found in a previous clonal analysis performed on samples taken from the Solfatara (Glamocclija *et al.* 2004a) and in various environments including shallow- and deep-sea vents (Sievert, Kuever and Muyzer 2000; Lopez-Garcia *et al.* 2003) and in soil after a geothermal heating event at Yellowstone National Park (Norris *et al.* 2002).

Verrucomicrobial methanotrophs were not detected in this study, although novel species of *Methylacidimicrobium* were recently discovered in the Solfatara Crater (van Teeseling *et al.* 2014). However, OTUs generically affiliated to the phylum *Verrucomicrobia* or specifically to genus *Chtoniobacter* were retrieved in our samples suggesting the possible presence of new methanotrophic *Verrucomicrobia*. Within *Chloroflexi*, it is worth noting the occurrence of OTUs, mainly not identified at genus level, belonging to the class *Ktedonobacteria*. Members of this class were previously isolated from geothermal soils (Yabe *et al.* 2010, 2011, 2017). Remarkably, the occurrence of OTUs not identified at genus level revealed a new microbial diversity within *Acidobacteria*, *Chloroflexi*, *Verrucomicrobia* and *Thaumarchaeota* phyla in such an extremely acidic environment, which deserves further investigation.

The combination of high-throughput sequencing with single-cells quantification assays provided a deep insight into biodiversity in the Solfatara Crater, highlighting some differences with previously well-studied, high-enthalpy geothermal systems, e.g. lack of evidence of members of *Aquificae* phylum typically reported in hyperthermophilic, alkaline systems such as Yellowstone National Park (Takacs-Vesbach *et al.* 2013). A wide distribution of different *Aquificales* lineages as a function of the geochemical conditions was reported for Yellowstone National Park, with the dominance of *Hydrogenobaculums* spp. specifically associated with the acidic, sulfidic sites (Takacs-Vesbach *et al.* 2013).

In this study, the integrated geochemical and microbiological characterization highlighted how the microbial communities are shaped by deep-originated gases and elements. Fumarolic gas emissions (rich in CO_2, CH_4 and H_2S), high temperature and acidity select microbial communities with high metabolic versatility as a strategy to deal with extreme reaction environments.

ACKNOWLEDGMENTS

Conflicts of interest

None declared.

References

Aliaga Goltsman DS, Comolli LR, Thomas BC *et al.* Community transcriptomics reveals unexpected high microbial diversity in acidophilic biofilm communities. *ISME J* 2015;**9**:1014–23.

Allard P, Maiorani A, Tedesco D *et al.* Isotopic study of the origin of sulfur and carbon in Solfatara fumaroles, Campi Flegrei caldera. *J Volcanol Geotherm Res* 1991;**48**:139–59.

Altschul SF, Gish W, Miller W *et al.* Basic Local Alignment Search Tool. *J Mol Biol* 1990;**215**:403–410.

Altschul SF, Madden TL, Schaffer AA *et al.* Gapped BLAST and PSI-BLAST: a new generation of protein database search programs. *Nucleic Acids Res* 1997;**25(17)**:3389–402.

Amalfitano S, Del Bon A, Zoppini A *et al.* Groundwater geochemistry and microbial community structure in the aquifer transition from volcanic to alluvial areas. *Water Res* 2014;**65**:384–94.

Arthur CL, Pawliszyn J. Solid phase microextraction with thermal desorption using fused silica optical fibers. *Anal Chem* 1990;**62**:2145–8.

Avrahamov N, Antler G, Yechieli Y *et al.* Anaerobic oxidation of methane by sulfate in hypersaline groundwater of the Dead Sea aquifer. *Geobiology* 2014;**12**:511–28.

Baker-Austin C, Dopson M, Wexler M *et al.* Extreme arsenic resistance by the acidophilic archaeon 'Ferroplasma acidarmanus' Fer1. *Extremophiles* 2007;**11**:425–34.

Benson CA, Bizzoco RW, Lipson DA *et al.* Microbial diversity in nonsulfur, sulfur and iron geothermal steam vents. *FEMS Microbiol Ecol* 2011;**76**:74–88.

Bruno PPG, Ricciardi GP, Petrillo Z *et al.* Geophysical and hydrogeological experiments from a shallow hydrothermal system at Solfatara Volcano, Campi Flegrei, Italy: Response to caldera unrest. *J Geophys Res* 2007;**112**:B06201.

Burton M.R, Sawyer GM, Granieri D. Deep carbon emissions from volcanoes. *Rev Mineral Geochem* 2013;**75**:323–54.

Caliro S, Chiodini G, Moretti R *et al.* The origin of the fumaroles of La Solfatara (Campi Flegrei, South Italy). *Geochim Cosmochim Acta* 2007;**71**:3040–55.

Cardellini C, Chiodini G, Frondini F *et al.* Accumulation chamber measurements of methane fluxes: application to volcanic-geothermal areas and landfills. *Appl Geochem* 2003;**18**:45–54.

Cardellini C, Chiodini G, Frondini F *et al.* Monitoring diffuse volcanic degassing during volcanic unrests: the case of Campi Flegrei (Italy). *Sci Rep* 2017;**7**:6757.

Chiodini G, Caliro S, Cardellini C *et al.* Carbon isotopic composition of soil CO2 efflux, a powerful method to discriminate different sources feeding soil CO2 degassing in volcanic-hydrothermal areas. *Earth Planet Sci Lett* 2008;**274**:372–9.

Chiodini G, Caliro S, Cardellini C *et al.* Long-term variations of the Campi Flegrei, Italy, volcanic system as revealed by the monitoring of hydrothermal activity. *J Geophys Res* 2010;**115**:B03205.

Chiodini G, Cioni R, Guidi M *et al.* Soil CO2 flux measurements in volcanic and geothermal areas. *Appl Geochem* 1998;**13**:543–52.

Chiodini G, Frondini F, Cardellini C *et al.* CO2 degassing and energy release at Solfatara volcano, Campi Flegrei, Italy. *J Geophys Res* 2001;**106**:16213–21.

Chiodini G, Giudicepietro F, Vandemeulebrouck J *et al.* Fumarolic tremor and geochemical signals during a volcanic unrest. *Geology* 2017;**45**:1131–4.

Chiodini G, Paonita A, Aiuppa A *et al*. Magmas near the critical degassing pressure drive volcanic unrest towards a critical state. *Nat Comms* 2016;**7**:13712.

Chiodini G, Pappalardo L, Aiuppa A *et al*. The geological CO_2 degassing history of a long-lived caldera. *Geology* 2015a;**43**:767–70.

Chiodini G, Vandemeulebrouck J, Caliro S *et al*. Evidence of thermal-driven processes triggering the 2005–2014 unrest at Campi Flegrei caldera. *Earth Planet Sci Lett* 2015b;**414**:58–67.

Christel S, Herold M, Bellenberg S *et al*. Multi-omics Reveals the Lifestyle of the Acidophilic, Mineral- Oxidizing Model Species Leptospirillum ferriphilum. *Appl Environ Microbiol* 2017;**84**:1–17.

Clarke KR. Non-parametric multivariate analyses of changes in community structure. *Austral Ecol* 1993;**18**:117–43.

Clum A, Nolan M, Lang E *et al*. Complete genome sequence of Acidimicrobium ferrooxidans type strain (ICPT). *Stand Genomic Sci* 2009;**1**:38–45.

Colman DR, Poudel S, Hamilton TL *et al*. Geobiological feedbacks and the evolution of thermoacidophiles. *ISME J* 2018;**12**:225–36.

Dopson M, Baker-Austin C, Hind A *et al*. Characterization of Ferroplasma isolates and Ferroplasma acidarmanus sp. nov., extreme acidophiles from acid mine drainage and industrial bioleaching environments. *Appl Environ Microbiol* 2004;**70**:2079–88.

Dopson M, Johnson DB. Biodiversity, metabolism and applications of acidophilic sulfur-metabolizing microorganisms. *Environ Microbiol* 2012;**14**:2620–31.

Edwards KJ, Bond PL, Gihring TM *et al*. An archaeal iron-oxidizing extreme acidophile important in Acid Mine Drainage. *Science* 2000;**287**:1796–9

Evans WC, White LD, Rapp JB. Geochemistry of some gases in hydrothermal fluids from the southern Juan de Fuca ridge. *J Geophys Res* 1998;**15**:305–13.

Fazi S, Amalfitano S, Pizzetti I. Efficiency of fluorescence in situ hybridization for bacterial cell identification in temporary river sediments with contrasting water content. *Syst Appl Microbiol* 2007;**30**:463–70.

Fazi S, Vázquez E, Casamayor EO *et al*. Stream hydrological fragmentation drives bacterioplankton community composition. Smidt H (ed.). *PLoS One* 2013;**8**:e64109.

Federico C, Corso PP, Fiordilino E *et al*. CO2 degassing at La Solfatara volcano (Phlegrean Fields): Processes affecting and of soil CO2. *Geochim Cosmochim Acta* 2010;**74**:3521–38.

Foesel BU, Nägele V, Naether A *et al*. Determinants of Acidobacteria activity inferred from the relative abundances of 16S rRNA transcripts in German grassland and forest soils. *Environ Microbiol* 2014;**16**:658–75.

Foulquier A, Volat B, Neyra M *et al*. Long-term impact of hydrological regime on structure and functions of microbial communities in riverine wetland sediments. *FEMS Microbiol Ecol* 2013;**85**:211–26.

Fritsche W, Hofrichter M. Aerobic degradation by microorganisms. In: Rehm HJ, Reed G (eds.) *Biotechnology: Environmental Processes II*. Weinheim: Wiley, 2008, 144–67.

Giggenbach WF. A simple method for the collection and analysis of volcanic gas samples. *Bull Volcanol* 1975;**39**:132–45.

Glamoclija M, Garrel L, Berthon J *et al*. Biosignatures and bacterial diversity in hydrothermal deposits of Solfatara Crater, Italy. *Geomicrobiol J* 2004a;**21**:529–41.

Glamoclija M, Garrel L, López-Garcia P. Hydrothermal deposits and extremophiles of the Solfatara Crater, Italy, as a possible analogue to Mars. *Geophys Res Abstracts* 2004b;**6**:04838.

Glamoclija M, Garrel L, López-Garcia P. The Solfatara Crater, Italy: Characterization of hydrothermal deposits, biosignatures and their astrobiological implication. 5th Lunar and Planetary Science Conference 2004c, March 15–19, League City, Texas, abstract no. 1227.

Golyshina OV, Yakimov MM, Lünsdorf H *et al*. Acidiplasma aeolicum gen. nov., sp. nov., a euryarchaeon of the family Ferroplasmaceae isolated from a hydrothermal pool, and transfer of Ferroplasma cupricumulans to Acidiplasma cupricumulans comb. nov. *Int J Syst Evol Microbiol* 2009;**59**:2815–23.

Gottsmann J, Rymer H, Berrino G. Unrest at the Campi Flegrei caldera (Italy): A critical evaluation of source parameters from geodetic data inversion. *J Volcanol Geotherm Res* 2006;**150**:132–45.

Greuter D, Loy A, Horn M *et al*. probeBase—an online resource for rRNA-targeted oligonucleotide probes and primers: new features 2016. *Nucleic Acids Res* 2016;**44**:D586–9.

Guo W, Zhang H, Zhou W *et al*. Sulfur metabolism pathways in Sulfobacillus acidophilus TPY, a gram-positive moderate thermoacidophile from a hydrothermal vent. *Front Microbiol* 2016;**7**:1–13.

Hammer Ø, Harper DAT, Ryan PD. Past: Paleontological statistics software package for education and data analysis. *Palaeontol Electron* 2001;**4**:9.

Hedrich S, Johnson DB. Acidithiobacillus ferridurans sp. nov., an acidophilic iron-, sulfur- and hydrogen-metabolizing chemolithotrophic gammaproteobacterium. *Int J Syst Evol Microbiol* 2013;**63**:4018–25.

Hippe H. Leptospirillum gen. nov. (ex Markosyan 1972), nom. rev., including Leptospirillum ferrooxidans sp. nov. (ex Markosyan 1972), nom. rev. and Leptospirillum thermoferrooxidans sp. nov. (Golovacheva *et al*. 1992). *Int J Syst Evol Microbiol* 2000;**50**:501–3.

Holmes AJ, Costello A, Lidstrom ME *et al*. Evidence that participate methane monooxygenase and ammonia monooxygenase may be evolutionarily related. *FEMS Microbiol Lett* 1995;**132**:203–8.

Hou W, Wang S, Dong H *et al*. A comprehensive census of microbial diversity in Hot Springs of Tengchong, Yunnan Province China Using 16S rRNA Gene Pyrosequencing. *PLoS One* 2013, DOI:10.1371/journal.pone.0053350.

Huber R, Huber H, Stetter KO. Towards the ecology of hyperthermophiles: biotopes, new isolation strategies and novel metabolic properties. *FEMS Microbiol Rev* 2000;**24**:615–23.

Hug K, Maher Wa, Stott MB *et al*. Microbial contributions to coupled arsenic and sulfur cycling in the acid-sulfide hot spring Champagne Pool, New Zealand. *Front Microbiol* 2014;**5**:1–14.

Huse SM, Dethlefsen L, Huber Ja *et al*. Correction: Exploring microbial diversity and taxonomy using SSU rRNA hypervariable tag sequencing. *PLoS Genet* 2008;**4**:e1000255.

Huse SM, Welch DBM, Voorhis A *et al*. VAMPS: a website for visualization and analysis of microbial population structures. *BMC Bioinformatics* 2014b;**15**:41.

Huse SM, Young VB, Morrison HG *et al*. Comparison of brush and biopsy sampling methods of the ileal pouch for assessment of mucosa-associated microbiota of human subjects. *Microbiome* 2014a;**2**:5.

Inagaki F, Nunoura T, Nakagawa S *et al*. Biogeographical distribution and diversity of microbes in methane hydrate-bearing deep marine sediments on the Pacific Ocean Margin. *Proc Natl Acad Sci* 2006;**103**:2815–20.

Inskeep WP, Rusch D, Jay Z *et al.* Metagenomes from high-temperature chemotrophic systems reveal geochemical controls on microbial community structure and function. *PLoS One* 2010;**5**:e9773.

Inskeep WP, Zackary JJ, Tringe SG *et al.* The YNP metagenome project: environmental parameters responsible for microbial distribution in the Yellowstone geothermal ecosystem. *Front Microbiol* 2013;**4**:1–15.

ISRIC (International Soil Reference and Information Centre). Procedures for soil analysis. Van Reeuwijk (ed.) 1995.

Jones DS, Albrecht HL, Dawson KS *et al.* Community genomic analysis of an extremely acidophilic sulfur-oxidizing biofilm. *ISME J* 2012;**6**:158–70.

Jones RD, Morita RY. Methane Oxidation by Nitrosococcus oceanus and Nitrosomonas europaea, *Appl Environ Microb* 1983;**45**:401–10.

Jones RT, Robeson MS, Lauber CL *et al.* A comprehensive survey of soil acidobacterial diversity using pyrosequencing and clone library analyses. *ISME J* 2009;**3**:442–53.

Kielak AM, Barreto CC, Kowalchuk GA *et al.* The ecology of Acidobacteria: moving beyond genes and genomes. *Front Microbiol* 2016;**7**:744.

Kilburn CRJ, De Natale G, Carlino S. Progressive approach to eruption at Campi Flegrei caldera in southern Italy. *Nat Comms* 2017;**8**:15312.

Kvist T, Ahring B, Westermann P. Archaeal diversity in Icelandic hot springs. *FEMS Microbiol Ecol* 2007;**59**:71–80.

Li H, Yang Q, Li J, Gao H *et al.* The impact of temperature on microbial diversity and AOA activity in the Tengchong Geothermal Field, China. *Sci Rep* 2015;**5**:17056.

Lin KH, Liao BY, Chang HW *et al.* Metabolic characteristics of dominant microbes and key rare species from an acidic hot spring in Taiwan revealed by metagenomics. *BMC Genomics* 2015;**16**:1–16.

Lopez-Garcıa P, Duperron S, Philippot P *et al.* Bacterial diversity in hydrothermal sediment and epsilonproteobacterial dominance in experimental microcolonizers at the Mid-Atlantic Ridge. *Environ Microbiol* 2003;**5**:961–76.

Mathur J, Bizzoco RW, Ellis DG *et al.* Effects of abiotic factors on the phylogenetic diversity of bacterial communities in acidic thermal springs. *Appl Environ Microbiol* 2007;**73**:2612–23.

Mayer K, Scheu B, Montanaro C *et al.* Hydrothermal alteration of surficial rocks at Solfatara (Campi Flegrei): Petrophysical properties and implications for phreatic eruption processes. *J Volcanol Geotherm Res* 2016;**320**:128–43.

Menzel P, Gudbergsdóttir SR, Rike AG *et al.* Comparative metagenomics of eight geographically remote terrestrial hot springs. *Microb Ecol* 2015;**70**:411–24.

Montanaro C, Mayer K, Isaia R *et al.* Hydrothermal activity and subsoil complexity: implication for degassing processes at Solfatara crater, Campi Flegrei caldera. *Bull Volcanol* 2017;**79**:83.

Montegrossi G, Tassi F, Vaselli O *et al.* Sulfur Species in Volcanic Gases. *Anal Chem* 2001;**73**:3709–15.

Norris TB, Wraith JM, Castenholz RW *et al.* Soil microbial community structure across a thermal gradient following a geothermal heating event. *Appl Environ Microbiol* 2002;**68**:6300–9.

O'Neill GG, Wilkinson JF. Oxidation of ammonia by methane-oxidizing bacteria and the effects of ammonia on methane oxidation. *J Gen Microbiol* 1977;**100**:407–12.

Peech M. Hydrogen-ion activity. In: Black CA *et al.*(Eds.) *Methods of Soil Analysis Part 2*. Madison: American Society of Agronomy, 1965, 914–26.

Piochi M, Mormone A, Balassone G *et al.* Native sulfur, sulfates and sulfides from the active Campi Flegrei volcano (southern Italy): Genetic environments and degassing dynamics revealed by mineralogy and isotope geochemistry. *J Volcanol Geotherm Res* 2015;**304**:180–93.

Quatrini R, Johnson DB. Microbiomes in extremely acidic environments: functionalities and interactions that allow survival and growth of prokaryotes at low pH. *Curr Opin Microbiol* 2018;**43**:139–47.

Rawlings DE, Tributsch H, Hansford GS. Reasons why 'Leptospirillum'-like species rather than Thiobacillus ferrooxidans are the dominant iron-oxidizing bacteria in many commercial processes for the biooxidation of pyrite and related ores. *Microbiology* 1999;**145**:5–13.

Roalkvam I, Jørgensen SL, Chen Y *et al.* New insight into stratification of anaerobic methanotrophs in cold seep sediments. *FEMS Microbiol Ecol* 2011;**78**:233–43.

Rognes T, Flouri T, Nichols B *et al.* VSEARCH: a versatile open source tool for metagenomics. *PeerJ* 2016;**4**:e2584.

Rojo F. Degradation of alkanes by bacteria. *Environ Microbiol* 2009;**11**:2477–90.

Sahm K, John P, Nacke H *et al.* High abundance of heterotrophic prokaryotes in hydrothermal springs of the Azores as revealed by a network of 16S rRNA gene-based methods. *Extremophiles* 2013;**17**:649–62.

Segerer A, Neuner A, Kristjansson JK *et al.* Acidianus infernus gen. nov., sp. nov., and Acidianus brierleyi Comb. nov.: Facultatively aerobic, extremely acidophilic thermophilic sulfur-metabolizing archaebacteria. *Int J Syst Bacteriol* 1986;**36**:559–64.

Sgavetti M, Pompilio L, Roveri M *et al.* Two geologic systems providing terrestrial analogues for the exploration of sulfate deposits on Mars: Initial spectral characterization. *Planet Space Sci* 2009;**57**:614–27.

Sicola S, Carapezza ML, Ranaldi M *et al.* Feasibility of high-frequency micro-gaschromatography soil gas monitoring revealed at La Solfatara (Campi Flegrei, Italy). 34°Convegno Nazionale GNGTS, Trieste, 17–19 novembre 2015, Atti del convegno, 158–63.

Sievert SM, Kuever J, Muyzer G. Identification of 16S Ribosomal DNA-Defined Bacterial Populations at a Shallow Submarine Hydrothermal Vent near Milos Island (Greece). *Appl Environ Microbiol* 2000;**66**:3102–9.

Stackebrandt E, Rainey FA, Ward-Rainey NL. Proposal for a New Hierarchic Classification System, Actinobacteria classis nov. *Int J Syst Bacteriol* 1997;**47**:479–91.

Stieglmeir M, Alves RJE, Schleper C. The Phylum Thaumarchaeota. In: Rosenberg E. *et al.*(eds.) *The Prokaryotes – Other Major Lineages of Bacteria and the Archaea*. Berlin Heidelberg: Springer, 2014, 10.1007/978-3-642-38954-2_338.

Stout LM, Blake RE, Greenwood JP *et al.* Microbial diversity of boron-rich volcanic hot springs of St. Lucia, Lesser Antilles. *FEMS Microbiol Ecol* 2009;**70**:402–12.

Takacs-Vesbach C, Inskeep WP, Jay ZJ *et al.* Metagenome sequence analysis of filamentous microbial communities obtained from geochemically distinct geothermal channels reveals specialization of three Aquificales lineages. *Front Microbiol* 2013;**4**:1–25

Tassi F, Bonini M, Montegrossi G *et al.* Origin of light hydrocarbons in gases from mud volcanoes and CH4-rich emissions. *Chem Geol* 2012;**294-295**:113–26.

Tassi F, Cabassi J, Calabrese S *et al*. Diffuse soil gas emissions of gaseous elemental mercury (GEM) from hydrothermal-volcanic systems: An innovative approach by using the static closed-chamber method. *Appl Geochem* 2016;**66**:234–41.

Tassi F, Nisi B, Cardellini C *et al*. Diffuse soil emission of hydrothermal gases (CO2, CH4, and C6H6) at Solfatara crater (Campi Flegrei, southern Italy). *Appl Geochem* 2013;**35**:142–53.

Tassi F, Venturi S, Cabassi J *et al*. Biodegradation of CO 2 , CH 4 and volatile organic compounds (VOCs) in soil gas from the Vicano–Cimino hydrothermal system (central Italy). *Org Geochem* 2015b;**86**:81–93.

Tassi F, Venturi S, Cabassi J *et al*. Volatile Organic Compounds (VOCs) in soil gases from Solfatara crater (Campi Flegrei, southern Italy): Geogenic source(s) vs. biogeochemical processes. *Appl Geochem* 2015a;**56**:37–49.

Topçuoğlu BD, Stewart LC, Morrison HG *et al*. Hydrogen limitation and syntrophic growth among natural assemblages of thermophilic methanogens at deep-sea hydrothermal vents. *Front Microbiol* 2016;**7**:1240.

Tunery CSM, Blockley SPE, Lowe JJ *et al*. Geochemical characterization of Quaternary tephras from the Campanian Province, Italy. *Quat Int* 2008;**178**:288–305.

Urbieta M, González Toril E, Aguilera A *et al*. First prokaryotic biodiversity assessment using molecular techniques of an acidic river in neuquén, argentina. *Microb Ecol* 2012;**64**:91–104.

Van Teesseling MCF, Pol A, Harhangi HR *et al*. Expanding the verrucomicrobial methanotrophic world: description of three novel species of Methylacidimicrobium gen. nov. *Appl Environ Microbiol* 2014;**80**:6782–91.

Vaselli O, Tassi F, Montegrossi G *et al*. Sampling and analysis of volcanic gases. *Acta Vulcanol* 2006;**18**:65–76.

Vaselli O, Tassi F, Tedesco D *et al*. Submarine and inland gas discharges from the Campi Flegrei (southern Italy) and the Pozzuoli Bay: geochemical clues for a common hydrothermal-magmatic source. *Procedia Earth and Planetary Science* 2011;**4**:57–73.

Venturi S, Tassi F, Bicocchi G *et al*. Fractionation processes affecting the stable carbon isotope signature of thermal waters from hydrothermal/volcanic systems: The examples of Campi Flegrei and Vulcano Island (southern Italy). *J Volcanol Geotherm Res* 2017a;**345**:46–57.

Venturi S, Tassi F, Gould IR *et al*. Mineral-assisted production of benzene under hydrothermal conditions: Insights from experimental studies on C 6 cyclic hydrocarbons. *J Volcanol Geotherm Res* 2017b, DOI: 10.1016/j.jvolgeores.2017.05.024.

Volant A, Desoeuvre A, Casiot C *et al*. Archaeal diversity: temporal variation in the arsenic-rich creek sediments of Carnoulès Mine, France. *Extremophiles* 2012;**16**:645–57.

Wang Q, Garrity GM, Tiedje JM *et al*. Naive Bayesian Classifier for rapid assignment of rRNA sequences into new bacterial taxonomy. *Appl Environ Microbiol* 2007;**73(16)**:5261–67.

Wemheuer B, Taube R, Akyol P *et al*. Microbial diversity and biochemical potential encoded by thermal spring metagenomes derived from the Kamchatka peninsula. *Archaea* 2013;**136**:714.

Wheaton G, Counts J, Mukherjee A *et al*. The confluence of heavy metal biooxidation and heavy metal resistance: implications for bioleaching by extreme thermoacidophiles. *Minerals* 2015;**5**:397–451.

Yabe S, Aiba Y, Sakai Y *et al*. *Thermogemmatispora onikobensis* gen. nov., sp. nov. and *Thermogemmatispora foliorum* sp. nov., isolated from fallen leaves on geothermal soils, and description of *Thermogemmatisporaceae* fam. nov. and *Thermogemmatisporales* ord. nov. within the class *Ktedonobacteria*. *Int J Syst Evol Microbiol* 2011;**61**:903–10.

Yabe S, Aiba Y, Sakai Y *et al*. *Thermosporothrix hazakensis* gen. nov., sp. nov., isolated from compost, description of *Thermosporotrichaceae* fam. nov. within the class *Ktedonobacteria* Cavaletti *et al*. 2007 and emended description of the class *Ktedonobacteria*. *Int J Syst Evol Microbiol* 2010;**60**:1794–801.

Yabe S, Sakai Y, Abe K *et al*. Diversity of *Ktedonobacteria* with actinomycetes-like morphology in terrestrial environments. *Microbes and environments* 2017;**32**:61–70.

Yelton AP, Comolli LR, Justice NB *et al*. Comparative genomics in acid mine drainage biofilm communities reveals metabolic and structural differentiation of co-occurring archaea. *BMC Genomics* 2013;**14**:485.

Zheng Y, Huang R, Wang BZ *et al*. Competitive interactions between methane- and ammonia-oxidizing bacteria modulate carbon and nitrogen cycling in paddy soil. *Biogeosciences* 2014;**11**:3353–68.